GRUPO ESPAÑOL CARBÓN
www.gecarbon.org

BOLETIN del Grupo Español del Carbón

ISSN 2172 - 6094
nº 31/Marzo 2014

INDICE

Editor Invitado:
José Rivera-Utrilla

Editorial

This special issue of the Boletín del Grupo Español del Carbón (Spanish Carbon Group Bulletin) focuses on the role of carbon materials in Advanced Oxidation Processes (AOPs) for water treatments. AOPs are defined as processes that involve the in situ generation of highly potent chemical oxidants such as hydroxyl radicals (HO•) in sufficient and optimum quantities to significantly enhance the oxidation and destruction of a wide range of organic pollutants in contaminated water and air. These free radicals are highly reactive species that can successfully attack most organic and inorganic compounds with very high reaction rate constants (10^6-10^9 M^{-1} s^{-1}). The numerous systems that can produce these radicals (Table 1) account for the high versatility of AOPs.

The progressive decline in water resources intended for human use and the increase in water consumption by industry, agriculture, and populations pose a challenge to conventional water treatment systems and their existing technology. However, conventional methods have proven unable to cope with the continuous emergence of new pollutants, prompting renewed research efforts to address the removal of these compounds from water reserves. More effective, efficient, and specific technologies for water treatment and pollutant removal are required. There is also a need for information systems, management models, and support procedures for decision-taking in order to rationalize water consumption and wastewater generation by integration and optimization strategies (e.g. reutilization, recycling) successfully utilized in engineering processes. Polluted water can generally be treated effectively by biological treatment plants using adsorbents or conventional chemical treatments (chlorination, ozonation, or permanganate oxidation). However, these procedures are sometimes unable to degrade pollutants to levels that are required by law or are essential for the subsequent use of the effluent. Research over the past few years has shown AOPs to be highly effective in the oxidation of numerous organic and inorganic compounds. AOP technologies are especially useful to remove biologically toxic or non-degradable pollutants such as aromatics, pesticides, petroleum constituents, pharmaceuticals, surfactants, colorants, and volatile organic compounds from wastewaters. Contaminant compounds are largely mineralized, by oxidation, into stable inorganic compounds such as carbon dioxide, water, and salts. One aim of the application of AOPs in wastewater treatments is to reduce chemical contaminants and water toxicity to a sufficient degree to allow reintroduction of the treated water into receiving streams or into a conventional sewage treatment plant.

The combination of the high efficiency of AOPs with the elevated adsorptive capacity of activated carbon or other carbon materials has recently been proposed as a highly attractive alternative to traditional AOPs. It has also been demonstrated that, in some cases, these carbon materials can act as initiators, promoters or catalysts of certain AOPs, increasing their effectiveness. Thus, a more effective pollutant degradation and mineralization and greater reduction in water toxicity were obtained by the simultaneous utilization of an AOP with a selected carbon material than by the AOP alone. Moreover, in several AOPs, carbon materials can be efficiently used as electrodes (electrochemical oxidation) or catalyst supports. This special issue of the Boletín del Grupo Español del Carbón provides an update on these novel roles of carbon materials in different AOPs: 1.- Catalytic wet peroxide oxidation (Authors: Prof. J. J. Rodríguez et al.). 2.- Electrochemical oxidation (Authors: Prof. E. Morallón et al.). 3.- Radiolysis (Authors: Prof. M. Sánchez-Polo et al.). 4.- Ozonation (Authors: Prof. M. F. R. Pereira et al.). 5.- Heterogeneous photocatalysis (Authors: Dr. C. O. Ania and Dr. L. F. Velasco). I am grateful to all authors for their kind efforts and excellent contributions to this issue.

José Rivera-Utrilla

Guest Editor

Table 1. Water treatment technologies based on Advanced Oxidation Processes

Non-photochemical processes	Photochemical processes
Oxidation in sub/supercritical water	Photolysis of water with vacuum UV
Catalytic wet peroxide oxidation	UV/hydrogen peroxide
Fenton's reagent (Fe^{2+}/H_2O_2)	UV/ozone
Electrochemical oxidation	Photo-Fenton
Radiolysis	Heterogeneous photocatalysis
Non-thermal plasma	
Ultrasound	
Ozonation in alkaline medium (O_3/OH^-)	
Ozonation in the presence of hydrogen peroxide (O_3/H_2O_2)	
Catalytic ozonation	

Aplicación de materiales carbonosos en Procesos de Oxidación Húmeda Catalítica con Peróxido de Hidrógeno

Carbon-based materials for Catalytic Wet Peroxide Oxidation Processes

A. Quintanilla, C.M. Domínguez, J.A. Zazo, J. A. Casas, J.J. Rodriguez

Sección de Ingeniería Química, Universidad Autónoma de Madrid

Corresponding author: *asun.quintanilla@uam.es*

Resumen

La Oxidación Húmeda Catalítica con Peróxido de Hidrógeno (Catalytic Wet Peroxide Oxidation, CWPO) constituye una tecnología emergente para la eliminación de contaminantes orgánicos recalcitrantes de las aguas, especialmente de efluentes industriales. Opera entre 25 y 130 ºC y a presión de 1-5 atm, empleando H_2O_2 como oxidante. El principal reto de este proceso, que limita su implantación industrial, es el desarrollo de catalizadores sólidos que combinen una buena actividad con una estabilidad que permita mantenerlos en operación por largos periodos con una alta eficiencia en el consumo de peróxido de hidrógeno. El presente trabajo resume algunos de los resultados obtenidos por el Grupo de Ingeniería Química de la Universidad Autónoma de Madrid (UAM) en la aplicación de esta técnica con catalizadores basados en materiales carbonosos, empleando fenol como compuesto tipo. Los catalizadores ensayados van desde metales soportados sobre carbón activado hasta los propios materiales carbonosos por sí mismos, incluyendo negros de humo y grafitos. La voltametría cíclica ha demostrado ser una técnica efectiva para evaluar la actividad de estos materiales en CWPO.

Abstract

Catalytic Wet Peroxide Oxidation (CWPO) relies on the oxidation of organic pollutants in water under mild operating conditions (T=25-130 ºC, P=1-5 atm) using hydrogen peroxide as oxidant. It represents an emerging technology whose main challenge, currently limiting its industrial application, is the development of catalysts capable of combining a good activity along with an adequate stability for long-term use and high efficiency of H_2O_2 consumption. This paper summarizes some of the results obtained by the Chemical Engineering Group of Universidad Autónoma de Madrid (UAM) on the application of that technique with carbon-based catalysts using phenol as target compound. The catalysts tested cover from metals supported on activated carbon to bare carbon materials including carbon blacks and graphites. Cyclic voltammetry has been successfully used to evaluate the activity of those materials in CWPO.

1. Introducción

La utilización intensiva del agua en la industria y el endurecimiento de los límites de vertido exigen el desarrollo de tecnologías cada vez más eficientes para el tratamiento de los efluentes residuales, especialmente en el caso de los contaminados por compuestos orgánicos recalcitrantes. En este sentido, los Procesos de Oxidación Avanzada (POAs), tratamientos en los que la materia orgánica es oxidada por especies radicalarias ($^{\cdot}OH$ y $^{\cdot}OOH$) en condiciones suaves de presión y temperatura (T=25-130 ºC, P=1-5 atm) constituyen una solución potencial. Debido a los costes asociados a las fuentes empleadas (O_3, H_2O_2, UV, etc.) para producir dichos radicales, los POAs son aplicables, generalmente, a niveles de contaminación orgánica correspondientes a valores de Demanda Química de Oxígeno (DQO) bajos o moderados [1].

El proceso de Oxidación Húmeda Catalítica con Peróxido de Hidrógeno (Catalytic Wet Peroxide Oxidation, CWPO) constituye uno de los POAs más efectivos y económicos. Se basa en la generación de radicales hidroxilo e hidroperóxido ($^{\cdot}OH$, $^{\cdot}OOH$) por la descomposición de peróxido de hidrógeno sobre la superficie de un catalizador:

$$Cat + H_2O_2 \rightarrow Cat^+ + {}^{\cdot}OH + OH^- \quad (1)$$

$$Cat^+ + H_2O_2 \rightarrow Cat + {}^{\cdot}OOH + H^+ \quad (2)$$

El tema ha recibido un interés creciente en las dos últimas décadas, como demuestra la evolución del número de artículos científicos publicados desde 1996, cuando aparece el primer trabajo sobre este proceso (Figura 1). Estos estudios están dedicados al tratamiento de diferentes compuestos orgánicos tóxicos y/o persistentes (*i.e.* fenol, derivados nitrogenados, clorados fenólicos y colorantes) mediante el empleo de diversos catalizadores sólidos [2].

Los catalizadores empleados suelen estar constituidos por una fase activa metálica anclada a la superficie de un sólido poroso, siendo la más estudiada el Fe (50% de los trabajos publicados, Figura 1), dada la elevada actividad que presenta este metal en la versión homogénea del proceso, bien conocido como oxidación Fenton. Otras fases activas, como Cu, Mn, Ni, Co y Au, han sido también empleadas, ya que presentan potenciales redox que, al igual que los del Fe, permiten la descomposición del H_2O_2 en radicales $^{\cdot}OH$ y $^{\cdot}OOH$ [3].

Los soportes catalíticos más empleados son arcillas, zeolitas, materiales silíceos, alúmina y materiales carbonosos. El empleo de estos últimos ocupa el 13% del total de trabajos publicados relativos al proceso CWPO (Figura 1), siendo el carbón activado el más utilizado. Esto es debido, por un lado, a sus propiedades texturales y su química superficial y, por otro, a su disponibilidad y economía en comparación con otros materiales. En menor medida, también se ha estudiado el empleo de aerogeles, resinas compuestas, nanofibras, nanotubos de carbón y diamante [2].

El principal reto del proceso CWPO es el desarrollo de catalizadores que combinen una buena actividad con la estabilidad que permita mantenerlos en servicio por un tiempo suficientemente largo, con una alta eficiencia en el consumo de peróxido de hidrógeno ($\eta=X_{COT}/X_{H2O2}$). Así, un buen número de trabajos se centra en la búsqueda de estrategias para evitar o minimizar su desactivación [2]. Una de las causas principales de la misma deriva de la lixiviación de la fase activa metálica [4], como consecuencia

de un débil anclaje de ésta al soporte o al empleo de condiciones de reacción que la favorecen. La deposición de materia orgánica sobre la superficie del catalizador contribuye también a su desactivación, aunque, en general, en menor medida.

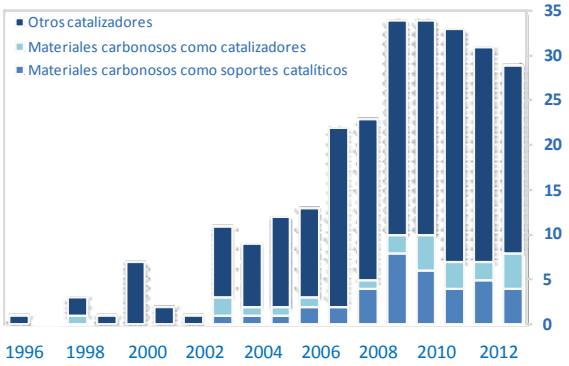

Figura 1. Evolución del número de publicaciones sobre el proceso CWPO.

Figure 1. Trend in the number of publications relative to CWPO.

Una alternativa razonable para evitar este problema es el empleo de catalizadores no metálicos, como los materiales carbonosos, con propiedades redox superficiales que permitan la descomposición del peróxido de hidrogeno. El 8% de los trabajos publicados en este campo está dedicado al empleo de este tipo de materiales directamente como catalizadores (Figura 1), siendo el carbón activado (52%) y el grafito (15%) los más empleados.

La preparación de catalizadores basados en materiales carbonosos, activos, eficientes y estables, y su aplicación en el tratamiento de aguas residuales contaminadas por compuestos persistentes mediante el proceso CWPO, constituye parte importante de la actividad investigadora del Grupo de Ingeniería Química de la Universidad Autónoma de Madrid, dentro de su línea de trabajo en el ámbito de la catálisis ambiental (www.iq-uam.es) . El presente artículo resume algunos de los resultados más significativos centrados en la oxidación de fenol como contaminante representativo.

2. Resultados y discusión

2.1. Desarrollo de catalizadores metálicos soportados sobre carbón activado

2.1.1. Catalizadores Fe/CA

Nuestros primeros estudios en este campo se centraron en el ensayo de catalizadores de hierro soportados sobre un carbón activado comercial (Merck ref.: 102514) por impregnación a humedad incipiente, utilizando nitrato de hierro como precursor [5]. En un principio el catalizador se preparó utilizando un 4% de fase activa y calcinándolo a 200ºC. Los resultados obtenidos (Figura 2) pusieron de manifiesto una alta actividad catalítica en la oxidación de fenol, alcanzándose conversión completa del mismo, con un grado de mineralización de hasta el 80% a pH 3 y 50ºC, con la cantidad estequiométrica de H_2O_2. Sin embargo, la formación de ácido oxálico entre los productos de reacción provoca una importante lixiviación de la fase metálica, lo que conduce a una rápida desactivación del catalizador, que mantiene una actividad residual en torno a un 40% de la inicial.

En un primer intento por mejorar la estabilidad del catalizador, el soporte se trató con ácido nítrico [6], para propiciar la formación de grupos oxigenados superficiales que pudieran mejorar el anclaje de la fase activa. Este tratamiento no afecta significativamente a la estructura porosa del catalizador. Los resultados obtenidos (Figura 2) indicaron un aumento significativo de la velocidad de oxidación, producto de una más rápida descomposición del H_2O_2. Este aumento de la actividad se debe a una mejor dispersión del hierro en la superficie del catalizador. Sin embargo, también aumentó la lixiviación del metal debido a una mayor concentración de ácido oxálico en el líquido, que forma un complejo con el Fe^{3+}, a tenor de la relación Fe/oxalato en la disolución.

Otra de las opciones estudiadas para mejorar la estabilidad del catalizador consistió en variar la temperatura en la etapa de calcinación (entre 150 y 300ºC) que sigue a la de impregnación [7]. Dentro del intervalo ensayado, se observó que dicha temperatura afecta a la naturaleza y distribución de los grupos oxigenados superficiales sin alterar significativamente las propiedades texturales. La actividad catalítica aumenta con la temperatura de calcinación (Figura 2), pero, paralelamente, la estabilidad se ve de nuevo comprometida por la formación de ácido oxálico. Similares resultados se obtuvieron empleando distintos precursores para la impregnación de la fase activa [8].

El avance más importante en esta línea se consiguió con un catalizador (Fe/C) preparado por activación química de lignina kraft con $FeCl_3$ [9], que mostró una menor actividad inicial pero con una alta estabilidad, corroborada frente a disoluciones de ácido oxálico

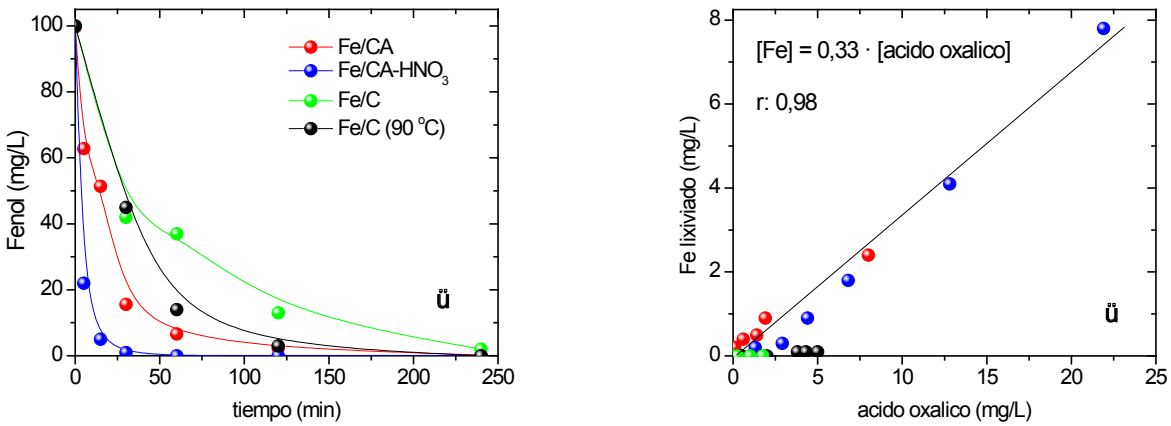

Figura 2. Evolución de la concentración de fenol en la oxidación con H_2O_2 mediante catalizadores Fe/CA y Fe/C (a) e influencia de la concentración de ácido oxálico sobre la lixiviación de hierro (b).

Figure 2. Phenol conversion upon CWPO with Fe/AC and Fe/C catalysts (a) and Fe leached vs. oxalic acid concentration (b).

sin lixiviación apreciable de Fe, lo que permite operar a temperatura más alta, con el consiguiente aumento de la actividad.

El procedimiento de preparación incluye una etapa inicial (lavado con ácido sulfúrico) para eliminar el contenido en cenizas de la lignina, que se impregna con $FeCl_3$, (1:1 en peso) y se activa en atmosfera inerte a 800ºC durante 2 horas [10]. La menor actividad inicial de este catalizador frente al Fe/CA puede explicarse por su contenido en Fe más bajo y una menor accesibilidad de los centros activos debido a su carácter casi exclusivamente microporoso.

2.1.2. Catalizadores Au/CA

Las nanopartículas de oro inmovilizadas sobre determinados soportes, *i.e.* diamante nanoparticulado, hidroxiapatita y carbón activado [11], se presentan como catalizadores interesantes para CWPO, gracias a su elevada resistencia a la lixiviación y a sus propiedades redox, que permiten catalizar la descomposición de H_2O_2 a especies radicalarias:

$$H_2O_2 + Au^0 \rightarrow \cdot OH + OH^- + Au^+ \quad (3)$$

$$H_2O_2 + Au^+ \rightarrow \cdot OOH + H^+ + Au^0 \quad (4)$$

Nuestro grupo ha estudiado la aplicación de estos catalizadores soportados sobre carbón activado [11, 12, 13]. En estos trabajos se observó un efecto sinérgico entre el oro y el soporte CA. Se consiguió un mejor aprovechamiento del H_2O_2, que permite obtener mayores grados de oxidación y mineralización, ya que el CA promueve la adsorción de fenol en las proximidades de las nanopartículas de oro, disminuyendo, por un lado, la velocidad de generación de especies radicalarias, al reducir el número de centros activos disponibles, y, por otro, aumentando la probabilidad de reacción entre los radicales formados y las moléculas de fenol. El estudio del efecto del tamaño de partícula del oro en la actividad del catalizador Au/CA en la oxidación de fenol (catalizadores preparados con distinto tamaño de partícula, por el método de impregnación-secado) permitió concluir que dicha variable presenta un efecto muy notable, de forma que cuanto menor es el tamaño de partícula, mayor es la actividad específica [11].

Atendiendo a un consumo eficiente de peróxido de hidrogeno, el empleo potencial de los catalizadores Au/CA debe limitarse al tratamiento de aguas residuales con una carga orgánica relativamente alta (C_{fenol}=1-5 g/L) y con relaciones másicas contaminante/catalizador también elevada (>0,4).

Bajo estas premisas, se desarrolló y verificó un modelo cinético que permite predecir las velocidades de descomposición de peróxido de hidrógeno y oxidación de fenol en un amplio intervalo de pH (3,5-7,5) [13]. El modelo incluye la desactivación del catalizador y el efecto de la temperatura. Su formulación se resume en las siguientes ecuaciones:

$$r_{H2O2}\left(\frac{g_{H2O2}}{L\cdot h}\right) = 5.447 \pm 2.58 \cdot e^{\frac{-30,33\pm2.66}{R\cdot T}} \cdot e^{-k_{d,H2O2}\cdot t} \cdot C_{H2O2} \quad (5)$$

$$r_{Fenol}\left(\frac{g_{Ph}}{L\cdot h}\right) = 61.635 \pm 34 \cdot e^{\frac{-45,78\pm9.14}{R\cdot T}} \cdot e^{-k_{d,Ph}\cdot t} \cdot C_{Fenol}^2 \quad (6)$$

La validez de dicho modelo se muestra en la Figura 3, en la que se presentan los resultados experimentales y predichos para la descomposición de peróxido de hidrógeno y la oxidación de fenol en distintas condiciones de operación.

La desactivación del catalizador Au/CA es debida al envenenamiento de la superficie de las partículas de Au por la adsorción de ácidos orgánicos, productos típicos de oxidación. Sin embargo, la actividad es fácilmente recuperable por un tratamiento térmico en atmosfera de aire a baja temperatura (200 ºC).

El catalizador Au/AC consigue, por tanto, superar las principales limitaciones de otros catalizadores sólidos empleados en CWPO, ya que no se produce la lixiviación de la fase activa y promueve un consumo eficiente de peróxido de hidrógeno (η=0,9 a 80 ºC); además permite trabajar con aguas residuales con un amplio intervalo de pH (3,5 -7,5). Sin embargo, para una completa eliminación del contaminante se requieren altos tiempos de reacción (22 h) y es necesario trabajar en ciclos de reacción-regeneración. La principal ventaja de este catalizador frente a otros estudiados en la bibliografía es que resulta posible recuperar la actividad catalítica fácilmente. No obstante, no parece suficiente para avalar, en la práctica, su empleo en procesos CWPO para la descontaminación de aguas.

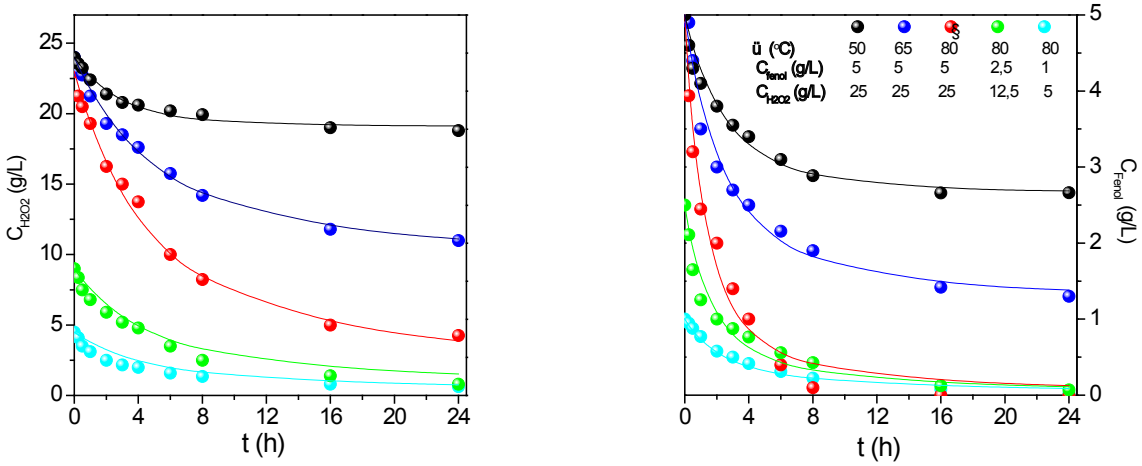

Figura 3. Resultados experimentales (símbolos) y predichos por el modelo (curvas) para la oxidación de fenol con H_2O_2 mediante el catalizador Au/CA.

Figure 3. Experimental (symbols) and predicted (curves) results from CWPO of phenol with Au/CA.

2.2. Empleo de materiales carbonosos como catalizadores

Una forma obvia de evitar los problemas derivados de la lixiviación de la fase metálica en los catalizadores para CWPO es prescindir de la misma. En este sentido hemos investigado el empleo directo de materiales carbonosos sin incorporación de componentes adicionales.

Se han ensayado tres tipos de materiales con propiedades diferentes: carbones activados (CA-M, ref.: 102514 y CA-P, ref.: 3108L), negros de humo (NH-C, ref.: 2156090 y NH-V, ref.: CC72R) y grafitos (G-S, ref.: 282863 y G-F, ref.: 1249167). Los carbones activados son materiales amorfos, con estructura porosa bien desarrollada y contenidos variables de grupos superficiales oxigenados (GSO). Por su parte, los grafitos son cristalinos, con bajo desarrollo superficial y prácticamente exentos de GSO, mientras que los negros de humo presentan propiedades intermedias entre ambos. Todos los materiales estudiados presentan muy bajo contenido en cenizas, exceptuando CA-M, con un 4% y G-S, con un 0,5%, en este último caso, correspondiente muy mayoritariamente a hierro.

2.2.1. Actividad catalítica en la reacción de descomposición de peróxido de hidrógeno

La voltametría cíclica, técnica de caracterización electroquímica con la que pueden medirse las propiedades redox de los materiales carbonosos, permite predecir de manera rápida, económica y sencilla la actividad de los mismos en la reacción de descomposición de peróxido de hidrógeno y poder, así, seleccionar potenciales catalizadores para el proceso CWPO. El reciente trabajo de Dominguez y col. [14] muestra que la corriente de intercambio del proceso global (i_o), parámetro electroquímico más representativo, ya que engloba las reacciones de oxidación y de reducción de peróxido de hidrógeno, se relaciona de forma lineal con la actividad de estos materiales, determinada por la constante cinética aparente de descomposición del peróxido de hidrógeno, k_d (Figura 4).

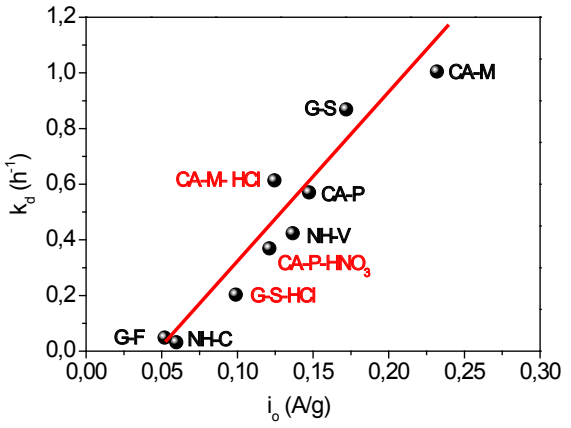

Figura 4. Relación entre la corriente de intercambio global (i_o) y la constante cinética de descomposición de H_2O_2 (k_d) para los materiales carbonosos ensayados.

Figure 4. Relationship between the current exchange (i_o) and the H_2O_2 decomposition (k_d) for the carbon materials tested.

2.2.1. Actividad, eficiencia y estabilidad de los materiales carbonosos en el proceso CWPO

Los CAs son catalizadores eficientes en el proceso CWPO sólo si se emplean en el tratamiento de aguas contaminadas por compuestos con alta afinidad por la superficie de los mismos, a concentraciones de materia orgánica relativamente altas (1-5 g/L) y relaciones de contaminante/carbón también altas (p.e. $C_{fenol}/C_{carbón} \geq 2$) [15]. En estas condiciones, la superficie específica de los CAs queda cubierta en una proporción adecuada para conseguir una velocidad de descomposición del H_2O_2 ajustada a las necesidades del proceso. Por otro lado, las moléculas de contaminante, al estar adsorbidas sobre el carbón, resultan fácilmente accesibles a los radicales (·OH, ·OOH) formados, aumentando la probabilidad de reacción. De este modo, se han obtenido eficiencias de consumo de oxidante muy altas (η=0,9-1), con una conversión prácticamente completa (>97% en el caso del fenol) y un alto grado de mineralización (70%) tras 24 h de reacción (catalizador CA-P de la Figura 5).

Este material (CA-P) sufre una progresiva desactivación con el número de ciclos de reacción (de 24 h cada uno) como muestra la Figura 6, debido a la adsorción de depósitos carbonosos sobre su superficie. No obstante, la actividad se recupera fácilmente mediante un tratamiento térmico a 350 ºC en atmósfera de aire. Por otro lado, dicha desactivación puede evitarse si los depósitos carbonosos son oxidados en el trascurso de la reacción. Esto es posible vía intensificación del proceso CWPO, alimentando oxígeno y aumentando la temperatura y presión de trabajo [16]. Los resultados obtenidos en un reactor de goteo son muy prometedores habiéndose alcanzado conversión completa de fenol y una reducción de COT del 70% a tiempos espaciales de 160 $g_{cat}\cdot h/g_{fenol}$, a 127 ºC y 8 atm con la dosis estequiométrica de peróxido de hidrógeno. Se comprobó la estabilidad de este catalizador durante 135 h de operación en continuo, aunque sí se observaron algunos cambios en el carbón, como una reducción del área específica y un incremento importante de la concentración de grupos oxigenados en la superficie.

Dado que la desactivación de los carbones activados en el proceso CWPO está estrechamente relacionada con su capacidad de adsorción, cabe esperar que materiales carbonosos con menor desarrollo superficial y, por tanto, menor capacidad de adsorción, como los negros de humo y los grafitos, presenten una mayor resistencia a la misma. Se estudió la actividad de NH-C y G-S en CWPO de fenol (Figura 5) [17]. En las condiciones de operación empleadas, el catalizador G-S condujo a mayores conversiones de fenol y COT (98% y 60%) que NH-C (60% y 35%, a las 4 h de reacción) como consecuencia, en gran parte, de la contribución homogénea del Fe en disolución, procedente de las cenizas del carbón. Debido a ello, G-S mostró una acusada pérdida de actividad del primer al segundo ciclo (Figura 6). Por el contrario, NH-C se mantuvo estable durante cinco usos consecutivos, con una eficiencia en el consumo de peróxido de hidrogeno superior a 0,9. Este material no contiene metales en su estructura y presenta una baja capacidad de adsorción. Se observó un aumento de su actividad en los primeros ciclos, gracias a un incremento del contenido de GSO, que mejora la difusión de los reaccionantes hacia los centros activos.

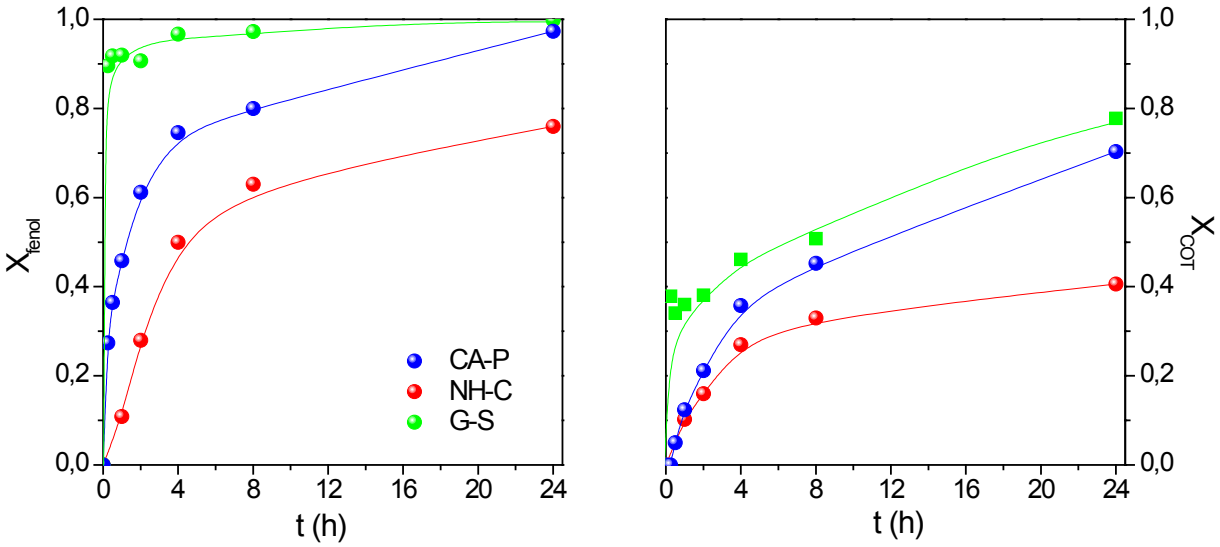

Figura 5. CWPO de fenol con distintos materiales carbonosos. Condiciones de operación: $C_{fenol,0}$=5 g/L, $C_{H2O2,0}$=25 g/L (CA-P), $C_{fenol,0}$=1 g/L, $C_{H2O2,0}$=5 g/L (NH-C y G-S), C_{cat}=2,5 g/L, T=80 ºC, pH_0= 3,5.

Figure 5. CWPO of phenol with different carbon materiales. Operating conditions: $C_{fenol,0}$=5 g/L, $C_{H2O2,0}$=25 g/L (CA-P), $C_{fenol,0}$=1 g/L, $C_{H2O2,0}$=5 g/L (NH-C y G-S), C_{cat}=2,5 g/L, T=80 ºC, pH_0= 3,5.

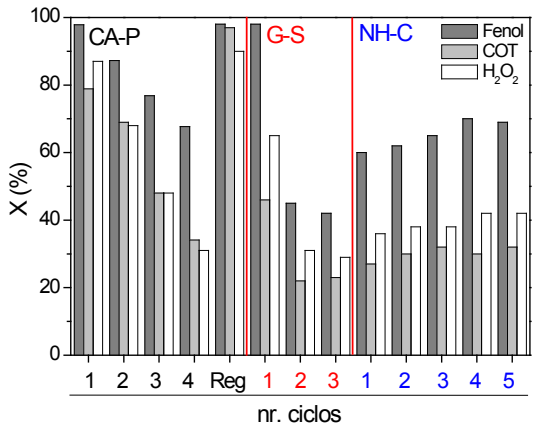

Figura 6. Estabilidad de los materiales carbonosos ensayados en ciclos consecutivos de 24 h. Condiciones de operación: $C_{fenol,0}$=1 g/L, $C_{H2O2,0}$=5 g/L, C_{cat}=2,5 g/L, T=80 ºC, pH_0= 3,5, t=4 h.

Figure 6. Performance of the carbon materials tested upon successive experiments of 24 h each at $C_{fenol,0}$=1 g/L, $C_{H2O2,0}$=5 g/L, C_{cat}=2,5 g/L, T=80 ºC, pH_0= 3,5 and t=4 h.

Por lo tanto, NH-C ha demostrado ser un catalizador activo, eficiente y estable para CWPO. El análisis de las condiciones de operación mostró que bajo las más adecuadas: C_{fenol}=1 g/L, C_{H2O2}=5 g/L, C_{cat}= 5 g/L, pH=3,5 y 90 ºC, es posible alcanzar conversión completa de fenol y una reducción de COT del 70%, en 16 h, con una eficiencia máxima en el consumo de peróxido de hidrógeno [19]. La actividad exhibida y, sobre todo, la eficiencia en el consumo de oxidante, con este tipo de catalizador, negro de humo, material que no ha sido estudiado con anterioridad, son muy elevadas en comparación con los resultados recogidos en la bibliografía para otros materiales carbonosos. Se trata, por tanto, de un catalizador prometedor para el tratamiento de aguas residuales industriales mediante CWPO. En la actualidad trabajamos en el desarrollo de un modelo cinético con vistas a su aplicación para el diseño del proceso CWPO para el tratamiento de aguas residuales reales, con las que venimos ensayando.

3. Agradecimientos

Las investigaciones resumidas en este trabajo han sido financiadas por el Ministerio de Ciencia e Innovación (Proyectos CTQ2008-03988 y CTQ2010-14807) y la Comunidad de Madrid (consorcio REMTAVARES, S2009/AMB-1588).

Nuestro agradecimiento a P. Ocón catedrática del Dpto. de Química-Física Aplicada de la UAM, y a los doctores S. Blasco y S. García por su colaboración que ha hecho posible la realización de este trabajo.

4. Referencias

[1] Matatov-Meytal YI, Sheintuch M. Catalytic abatement of water pollutants. Ind. Eng. Chem. Res.1998; 37: 309-26.

[2] Domínguez CM. Catalizadores basados en materiales carbonosos para procesos de oxidación húmeda con peróxido de hidrógeno. Universidad Autónoma de Madrid. Tesis Doctoral 2014.

[3] Aguado J. Tratamientos avanzados de aguas residuales industriales. Universidad Rey Juan Carlos, Colección Ciencias Experimentales y Tecnología 2012.

[4] Rokhina EV, Virkutyte J. Environmental Application of Catalytic Processes: Heterogeneous Liquid Phase Oxidation of Phenol With Hydrogen Peroxide. Crit. Rev. Env. Sci. Technol. 2012; 41: 125-167.

[5] Zazo JA, Casas JA, Mohedano AF, Rodríguez JJ. Catalytic wet peroxide oxidation of phenol with a Fe/Active carbon catalyst. App. Catal. B Environ. 2006; 65: 261-268

[6] Zazo JA, Casas JA, Mohedano AF, Rodriguez JJ. Improvement of Fe/activated carbon catalyst for CWPO upon oxidative treatment. Proceedings of Carbon Conference, 2008.

[7] Zazo JA, Fraile AF, Rey A, Bahamonde A, Casas JA, Rodriguez JJ. Optimizing calcination temperature of Fe/activated carbon catalysts for CWPO. Catal. Today 2009; 143: 341-346.

[8] Rey A., Faraldos M, Casas JA, Zazo JA, Bahamonde A, Rodriguez JJ. Catalytic wet peroxide oxidation of phenol over Fe/ac catalysts: influence of iron precursor and Activated carbon surface. App. Catal. B Environ. 2009; 86: 69-77.

[9] Zazo JA, Bedia J, Fierro CM, Pliego G, Casas JA, Rodriguez JJ. Highly stable Fe on activated carbon

catalysts for CWPO upon $FeCl_3$ activation of lignin from black liquors. Catal. Today 2012; 187(1): 115-121.

[10] Rodriguez JJ, Zazo JA, Fierro CM, Bedia J, Casas JA. Procedimiento de obtención de catalizadores de hierro soportado sobre carbón activo. Patente española, 201131674. 18 de octubre de 2011.

[11] Quintanilla A, Garcia-Rodriguez S, Dominguez CM, Blasco S, Casas JA, Rodriguez JJ. Supported gold nanoparticle catalysts for wet peroxide oxidation. App. Catal. B Environ. 2012; 111: 81-89.

[12] Quintanilla A, Dominguez, CM Blasco, S Casas, JA Rodriguez, JJ. Catalytic Wet Peroxide Oxidation of Organic Pollutants by Gold. 2nd European conference on Environmental Applications of Advanced Oxidation Processes 2009.

[13] Domínguez CM., Quintanilla A, Casas JA, Rodriguez JJ. Kinetics of wet peroxide oxidation of phenol with a gold/activated carbon catalyst. Chem. Eng. J. *Submitted*.

[14] Domínguez CM, Ocón P, Quintanilla A, Casas JA, Rodriguez JJ. The use of cyclic voltammetry to assess the activity of carbon materials for hydrogen peroxide decomposition. Carbon 2013; 60: 76-83.

[15] Domínguez CM, Ocón P, Quintanilla A, Casas JA, Rodriguez JJ. Highly efficient application of activated carbon as catalyst for wet peroxide oxidation. Appl. Catal. B Environ. 2013; 140–141 (0): 663-670.

[16] Quintanilla A, Fraile A, Casas JA, Rodríguez JJ. Phenol oxidation by a sequential CWPO–CWAO treatment with a Fe/AC catalyst. J. Hazard. Mater. 2007; 146: 582-588.

[17] Domínguez CM, Ocón P, Quintanilla A, Casas JA, Rodriguez JJ. Graphite and carbon black materials as catalysts for wet peroxide oxidation. Appl. Catal. B Environ. 2014; 144: 599-606.

Synthetic Boron-Doped Diamond Electrodes for Electrochemical Water Treatment

Electrodos de Diamante Dopado con Boro para el tratamiento electroquímico de aguas

F. Montilla, A. Gamero-Quijano, E. Morallón.

Departamento de Química Física. Instituto Universitario de Materiales. Universidad de Alicante. Apartado de Correos 99. 03080 Alicante (Spain). http://web.ua.es/electro/.

Abstract

Boron-doped diamond electrodes have emerged as anodic material due to their high physical, chemical and electrochemical stability. These characteristics make it particularly interesting for electrochemical wastewater treatments and especially due to its high overpotential for the Oxygen Evolution Reaction. Diamond electrodes present the maximum efficiency in pollutant removal in water, just limited by diffusion-controlled electrochemical kinetics. Results are presented for the elimination of benzoic acid and for the electrochemical treatment of synthetic tannery wastewater. The results indicate that diamond electrodes exhibit the best performance for the removal of total phenols, COD, TOC, and colour.

Resumen

Los electrodos de diamante dopados con boro han surgido como un nuevo material anódico debido a su propiedades como estabilidad física, química y electroquímica. Estas características hacen a estos electrodos especialmente interesantes para el tratamiento electroquímico de aguas residuales, debido sobre todo a su elevado sobrepotencial para la reacción de formación de oxígeno. Los electrodos de diamante presentan una eficiencia máxima para la eliminación de contaminantes en el agua, sólo limitada por la cinética del proceso electroquímico controlado por difusión. Se muestran algunos ejemplos como en la eliminación de ácido benzoico y en el tratamiento electroquímico de aguas sintéticas del curtido de pieles. Los resultados indican que los electrodos de diamante muestran el mejor rendimiento para la eliminación de fenoles, DQO, COT, y del color.

1. Introduction

Carbon materials have been widely used in both analytical and industrial electrochemistry from early in the 19th century [1]. These type of electrodes present several advantages: low cost, wide potential window, relatively inert electrochemistry, and electrocatalytic activity for a variety of redox reactions. The electrochemical applications of carbon electrodes are well known: metal production, energy storage in batteries and supercapacitors, and catalyst supports. The classical materials for electrochemical application are graphite, glassy carbon, and carbon black, and some extensive reviews can be found in the literature [2, 3].

Newer carbon-based material with outstanding electrochemical properties is diamond electrodes. Completely sp^3 hybridized, tetrahedral bonding of diamond produces materials with high hardness and low electrical conductivity. Crystalline diamond is a wide bandgap semiconductor, with a gap higher than 6 eV in a single crystal, and therefore an electrical insulator. However, the introduction of dopant atoms in the structure (usually boron or nitrogen) induces electrical conductivity.

2. Diamond electrodes: Synthesis and characterization

The first publication on conductive diamond is due to Pleskov et al. in 1987 [4]. Since then, there have been a large number of publications on this field. Some reviews collect the results obtained in applying these electrodes to various fields of electroanalysis, photoelectrochemistry, electrocatalysis, etc. [2]

Diamond electrodes are usually obtained by hot filament assisted chemical vapor deposition (HF-CVD) on a support heated to about 800-850 ºC. Silicon is the most suitable support, but diamond has been grown on metals such as W, Mo , Ti , Nb, etc. The precursor gas is usually a mixture of a volatile organic compound (methane, acetone, methanol, etc.) and hydrogen.

The most widely used dopant is boron, conferring a p-type semi-conducting character to diamond. The boron source can be a volatile compound introduced into the reactant gases, such as trimethyl borate or B_2H_6, or solid boron located near the substrate during growth of the diamond film. The boron doping level is often in the range of 10^{18}-10^{20} atoms/cm^3 or a B/C ratio of about 10^{-5} to 10^{-3}. Boron doped diamond (BDD) has randomly oriented microcrystallites with facets and grain boundaries characteristic of a polycrystalline material.

Figure 1a shows a micrograph obtained with scanning electron microscopy of a Si/BDD electrode showing the typical morphology of these polycrystalline diamond electrodes. Depending on the preparation procedure, the crystallite size may vary between 0.2 and 40 μm approximately.

Polycrystalline diamond films prepared in these conditions contain small amounts of sp^2 carbon usually located in the grain boundaries, as verified by Raman spectroscopy [5]. Diamond electrodes exhibit a 1332 cm^{-1} phonon band. The line width of this band and changes in smaller features of the diamond Raman spectrum are indicators of crystallinity and purity of diamond films [6].

This diamond band is used extensively to evaluate the relative amounts of sp^3 and sp^2 hybridized carbon in diamond electrodes. The 1360 cm^{-1} intensity relative to the 1332 cm^{-1} band is a sensitive indicator of sp^2 impurities in natural or synthetic diamond, since Raman cross section for sp^2 carbon is approximately 50 times that of sp^3 carbon. Boron doping at the high levels results in observable changes in the symmetry of the 1332 cm^{-1} Raman band, which can be used to determine the doping level [7].

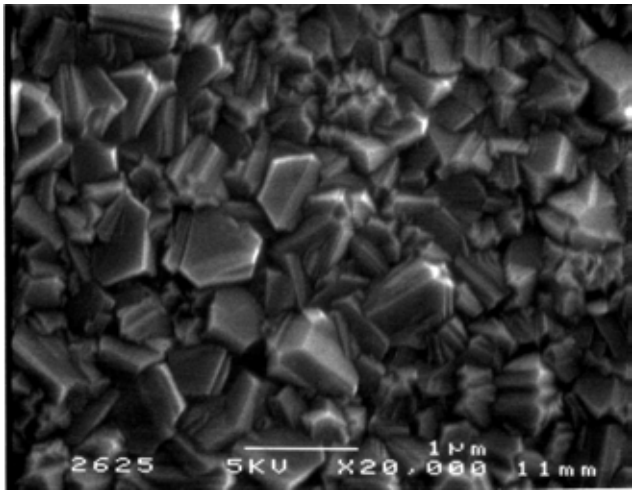

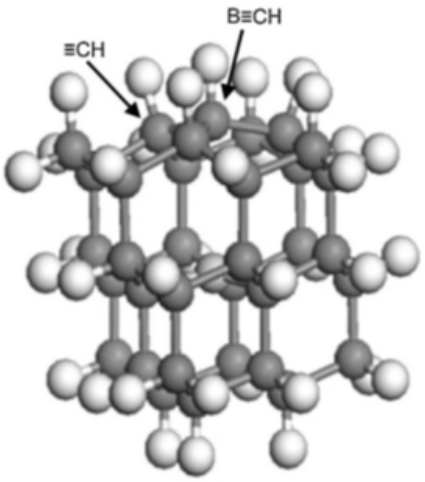

Figure 1. a) SEM images of a BDD film deposited on a silicon wafer. b) Simulated structure of a BDD. Hydrogen (white)-terminated diamond structure containing carbon and boron atoms.

Figura 1. a) Imágenes SEM de un depósito de BDD sobre Si, b) estructura simulada de BDD. Estructura de diamante conteniendo átomos de carbono, boro e hidrógeno (blancos).

3. Electrochemistry of diamond electrodes

BDD electrodes shows greater chemical stability compared with common sp^2 hybridized carbon electrode materials (i.e., graphite and glassy carbon electrodes). In addition to a long lifetime, the low chemical reactivity results in a wider electrochemical potential window.

Figure 2 shows cyclic voltammograms of a BDD electrode immersed in an aqueous solution, containing perchloric acid as supporting electrolyte.

In the high-scale potential range (figure 2, top), BDD electrode has a very wide electrochemical stability window that reach up to +2.5V at positive potentials. Above that potential the Oxygen Evolution Reaction (OER) takes place. This very high overpotential for OER makes this electrode very suitable for electrochemical degradation of organic compound, and also for electroanalysis.

Figure 2, bottom, shows the comparison between a BDD electrode and a graphite electrode. It can be observed that the BDD electrode is characterized by a low current density in the double layer charge, if compared to the capacitive current obtained with graphite electrode. The oxidation process observed at 1.9V has been related to the reactivity of non-diamond carbon species (sp^2 carbon) or impurity situated in the grain boundaries of the diamond surface. Undoped diamond has no electronic states within its band gap, which covers most of the electrochemical potential scale. Boron doping introduces “midgap” states that increase conductivity and electron transfer rates. In

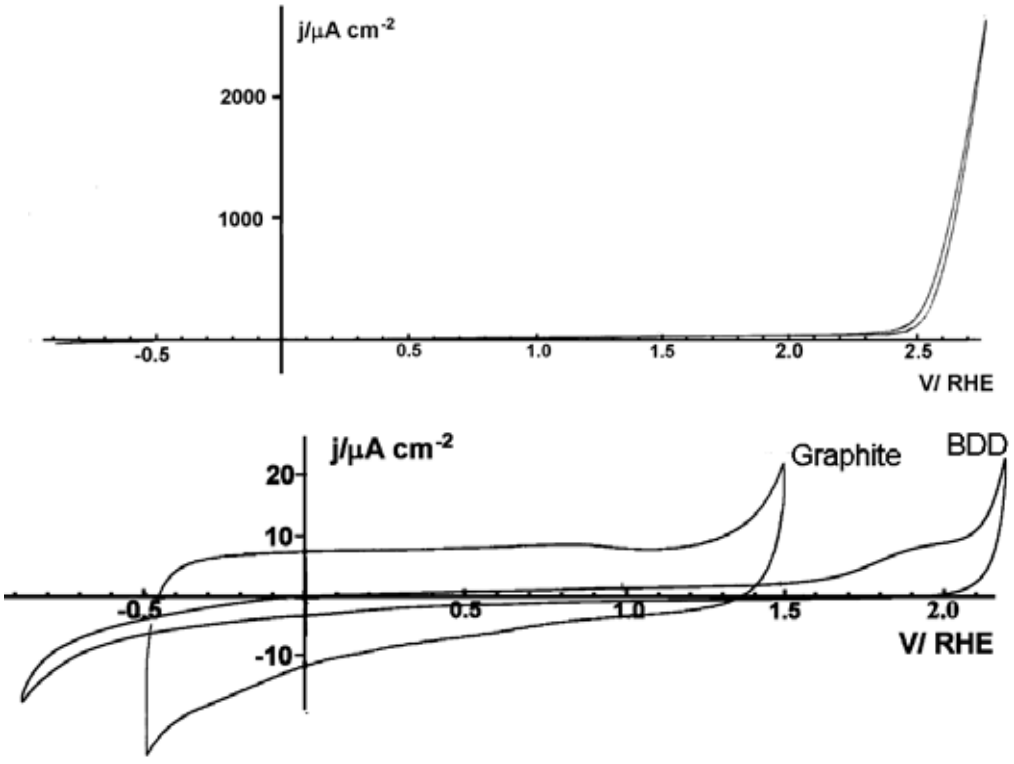

Figure 2. Cyclic voltammograms in aqueous 0.1M perchloric acid solution of a BDD diamond electrode (figure on top) and comparison between a BDD electrode and a graphite electrode (figure on bottom).

Figure 2. Voltagramas cíclicos de un electrodo BDD en ácido perclórico 0.1M (figura de arriba) y comparación entre un electrodo de BDD y un electrodo de grafito (figura de abajo).

that manner BDD is able to transfer electrons to most of the common redox probes, as showed in figure 3.

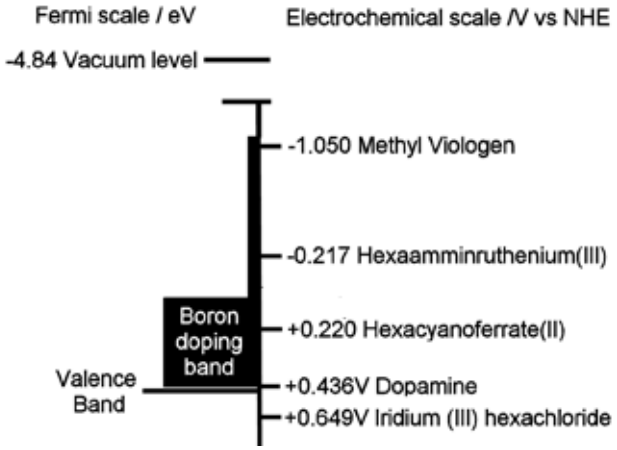

Figure 3. Energy states in BDD compared with the redox potentials of usual redox probes.

Figura 3. Estados energéticos del BDD comparados con los potenciales redox de diferentes pares redox.

The electrochemistry of organic compounds on BDD electrodes depends on the nature of surface adsorption. Standard redox probes have been studied on BDD electrodes in order to check the intrinsic electrocatalytic activity of this surface. As indicated by McCreery diamond electrodes has not adsorption sites and present a low electron transfer rate for redox as dopamine that requires adsorption, while methyl viologen voltammogram on BDD is quite similar to that on GC, since that compound can be considered as outer-sphere probe [2].

The intrinsic electrocatalytic activity of diamond, due to its lack of adsorption sites is low, but due to its inertness and low background currents this electrode is particularly interesting for fundamental studies on the electroactive compounds. The boron doped diamond electrode (BDD) is a suitable support for the characterization of electrocatalyst due to its high chemical and electrochemical stability, low background current, large electrochemical window and high thermal stability [8, 9].

4. Diamond electrodes, ideal anodes for electrochemical wastewater treatments

One of the most suitable treatments which can be performed on an effluent containing highly pollutants is the direct anodic oxidation (the so-called electrochemical incineration). In this process the electrode material must have a high efficiency of organic compounds oxidation, as well as a good stability under anodic polarization. A suitable model for understanding the processes of oxidation of organic compounds should also take into account the competitive reaction which occurs during the anodic oxidation of the organic compound, which is the Oxygen Evolution Reaction (OER).

The mechanism of electrochemical production of oxygen in aqueous media has been widely studied and different mechanisms have been proposed. There is a common initial step: a one-electron transfer to the solvent and the generation of an OH• radical in an active site surface electrode:

$$A_{(s)} + H_2O_{(l)} \rightarrow A_{(s)}(OH\bullet_{(ads)}) + H^+_{(aq)} + e^-_{(s)}$$

Being *A* the active site of the electrode. The following steps of the mechanism depends on the nature of the electrode used, concretely on its affinity for the OH• formed. At this point we can identify two types of mechanism, depending on whether the oxygen species is weakly adsorbed (physisorbed) or strongly adsorbed (chemisorbed) on the electrode. If the hydroxyl radical is physisorbed, the OH• is released to the solution where forms oxygen:

$$OH\bullet_{(aq)} \rightarrow O_{2(g)} + 2H^+_{(aq)} + 2e^-_{(s)}$$

A reaction intermediate of this step is the formation of a peroxide radical (O_2•) and it requires an important accumulation of physisorbed hydroxyl radicals and takes place at the potential of the H_2O/H_2O_2 redox couple (+1.77V/NHE). The production of oxygen by this route is not influenced by the chemical nature of the surface of the electrodes, because the chemical state of the electrode is not modified by the electron transfer reaction, but provides a physical adsorption site for the OH• radical. These electrodes are called "non-active" electrodes. This behavior is typical of electrode materials with absence of electroactive sites in the range of potentials between the thermodynamic potential for oxygen production (+1.23V/NHE) and the potential of H_2O/H_2O_2 redox couple, i.e. metal oxides in the highest oxidation state (such as PbO_2 or SnO_2). BDD electrode presents no redox active sites in that range of potentials and can be classified as non-active electrode (see figure 2).

These non-active electrodes present high overpotentials for the OER and therefore they are suitable electrodes for electrochemical oxidation-incineration of organic pollutants in industrial wastewaters, being the next reaction the final oxidation of a generic organic compound (R):

$$OH\bullet_{(aq)} + R_{(aq)} \rightarrow xCO_2 + yH_2O + H^+ + e^-$$

This reaction takes place at high overpotential, and the generation of OH• at high concentration favors the selective oxidation of organic, to give mainly CO_2. This electrode is also suitable for the electrochemical production of reactive oxidants such as ozone and hydrogen peroxide, because of their high OER overpotential. A model proposed by Comninellis et al. is useful for predicting the efficiency of electrochemical oxidation of organic compounds with "pure" non-active electrodes [10, 11]. It permits the prediction of the chemical oxygen demand (COD) and instantaneous current efficiency (ICE) during the electrochemical oxidation of organic pollutants on Si/BDD electrodes in a batch recirculation system under galvanostatic conditions.

The model supposes that the electrochemical oxidation-incineration of an organic compound is complete to CO_2, due to electrogenerated active intermediates formed by water discharge (OH radicals). The reaction between the OH radicals and the organic compound is considered much faster than the mass transport of the organic compound towards the anode.

Under these conditions, the limiting current density for the electrochemical incineration can be related to a global parameter of the solution, the Chemical Oxygen Demand (COD):

$$j_{lim}(t) = 4Fk_mCOD(t)$$

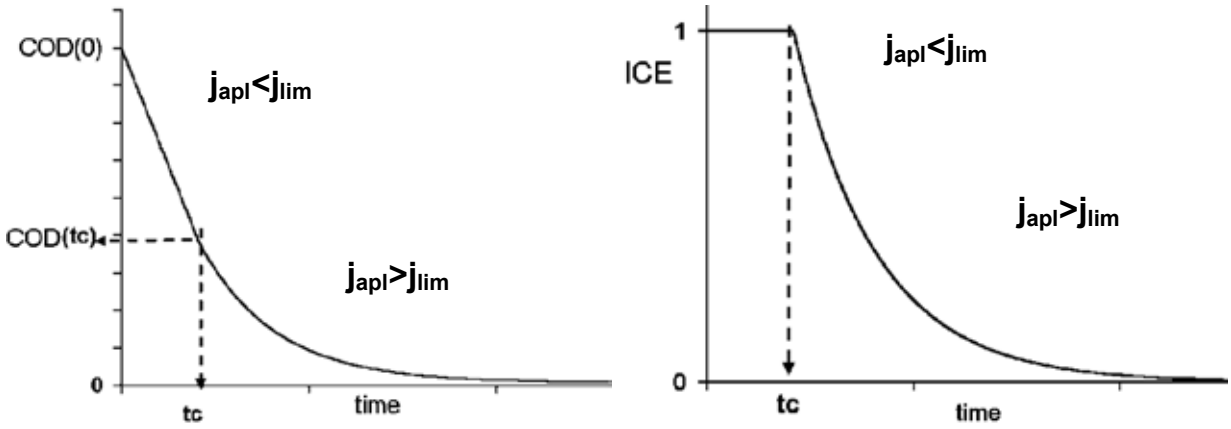

Figure 4. Evolution of the Chemical Oxygen Demand (COD) and Instantaneous Current Efficiency (ICE) as a function of time predicted by the Comninellis model during the galvanostatic oxidation of organic compounds in aqueous solution.

Figura 4. Variación de la demanda química de oxígeno (COD) y eficiencia en corriente instantánea (ICE) con el tiempo de electrolisis según el modelo de Comninellis durante una oxidación galvanostática de compuestos orgánicos en disolución acuosa.

Where $j_{lim}(t)$ is the limiting current density (A m^{-2}) at a given time t, *F* is the Faraday constant (C mol^{-1}), k_m is the average mass transport coefficient in the electrochemical reactor (m s^{-1}) and COD(t) is the chemical oxygen demand in the electrolyte at a given time t. This equation is valid for the electrooxidation of any organics and even when the solution contains more than one compound.

Depending on the applied current density (j_{appl}), two different operating regimes are identified: (i) $j_{appl.} < j_{lim}$: the electrolysis is under current control, the current efficiency is 100% and COD decreases linearly with time; (ii) $j_{appl.} > j_{lim}$: the electrolysis is under mass transport control and secondary reactions (such as oxygen evolution) start, resulting in a decrease of ICE. In this last regime, COD removal due to mass-transport limitation follows an exponential trend. The equations that describe the temporal trends of COD and ICE in both regimes are summarized in Table 1 and the expected evolution with time of COD and ICE during the electrochemical oxidation during the electrolysis at constant current is shown in figure 4.

As example, Figure 5 shows the evolution with time of COD and ICE during the electrochemical oxidation of different solutions of benzoic acid at constant current. Electrolysis at high anodic potentials in the region of electrolyte decomposition causes complex oxidation reactions that lead to the quasi complete incineration of BA. There is no indication of electrode fouling. In the inset of Figure 5, the theoretical value of COD and current efficiency trends calculated from the model (Table 1) are reported with the electrical charge. As predicted from the model, at the beginning of the electrolysis and at high benzoic acid concentration (8.86 mM, COD =2500 ppm), the reaction is under current limiting control ($j<j_{lim}$). This result in an instantaneous current efficiency (ICE) of almost 100% and in a linear decrease of COD with the specific charge passed. After some time of electrolysis, the COD in the solution decreased until a critical value, $COD(t_C)$ is achieved after this value both ICE and COD decrease exponentially with the specific charge passed as predicted by the model [12].

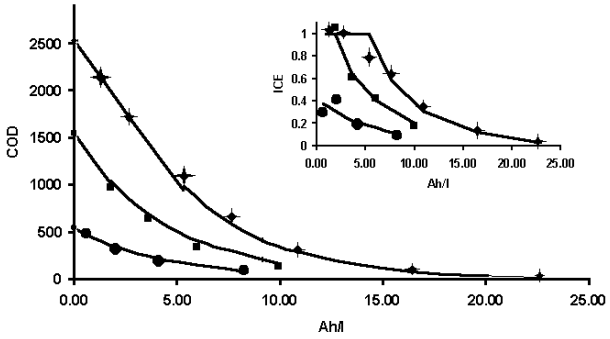

Figure 5. Evolution of COD and ICE (inset) during electrolysis of benzoic acid in 0.5M $HClO_4$. Initial concentration of benzoic acid, (✦) 8.86 mM, (■) 4.76 mM, (●) 2.11 mM. Anode: Boron-doped diamond electrode. Zr plate as cathode. T=25 °C. j= 24 mA cm^{-2}. The solid lines represent the model prediction.

Figura 5. Variación de la demanda química en oxígeno (COD) y la eficiencia en corriente instantánea (ICE)(figura insertada) en la oxidación de ácido benzoico en $HClO_4$ 0.5M , (✦) 8.86 mM, (■) 4.76 mM, (●) 2.11 mM. Ánodo: Electrodo de diamante dopado con boro. Cátodo: Zr. T=25 °C. j= 24 mA cm^{-2}. Las líneas sólidas correspondes a la simulación según el modelo.

Table 1. Equations that describe instantaneous current efficiency (ICE) and chemical oxygen demand (COD) during benzoic acid oxidation at Si/BDD electrode in acid solution.

Tabla 1. Ecuaciones que describen la eficiencia en corriente instantánea y la demanda química de oxígeno (COD) durante la oxidación de ácido benzoico con un electrodo Si/BDD en disolución ácida.

	Instantaneous current efficiency ICE	**Chemical Oxygen Demand COD ($molO_2$ m^{-3})**
under current control $j_{applied} < j_{limit}$	$ICE(t) = 1$	$COD(t) = COD(0)\left(1 - \frac{\alpha A k_m}{V_R} t\right)$
under mass transport control $j_{applied} > j_{limit}$	$ICE(t) = \exp\left(-\frac{A k_m}{V_R} t + \frac{1-\alpha}{\alpha}\right)$	$COD(t) = \alpha COD(0) * \exp\left(-\frac{A k_m}{V_R} t + \frac{1-\alpha}{\alpha}\right)$

Being $\alpha = j_{appl}/j_{lim(t=0)}$ and V_R the volume of the treated water

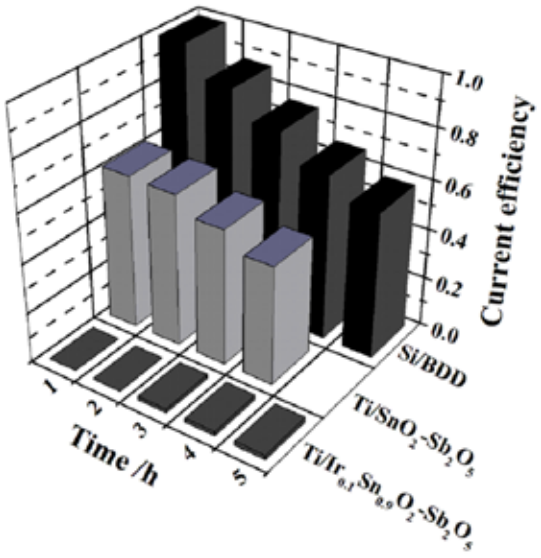

Figure 6. Current efficiency for the electrochemical incineration of tannery wastes with different anodes.

Figura 6. Eficiencia en corriente de la eliminación electroquímica de aguas sintéticas procedentes del curtido de pieles usando diferentes ánodos.

In similar manner, the electrochemical oxidation of other organic compounds on BDD anode demonstrates that the performance of this electrode is excellent, not only in the removal of pure refractory organic compounds [13], but also in complex mixtures of pollutants like in the electrochemical treatment of a synthetic tannery wastewater prepared with several compounds used by finishing tanneries. Results showed that faster removals of these parameters occurred when the Si/BDD was used as anode in comparison with other highly efficient anodes such as Ti/SnO_2Sb (see figure 6). This electrode was also the more efficient to remove the wastewater color [14].

Table 2 shows total organic carbon (TOC) removal and energy consumption after 4 h of electrochemical treatment of the synthetic tannery wastewater under different conditions. The Si/BDD anode is energetically more efficient than the other electrodes because it leads to faster TOC removal with lower energy consumption, although good results in terms of energy consumption are also obtained with the Ti/SnO_2–Sb anode. However, the latter anode has limited applicability because of its low stability. The increase in current density in the case of the Si/BDD anode results in faster wastewater mineralization with higher energy consumption.

Table 2. TOC removal and energy consumption obtained after 4 h of electrochemical treatment of the synthetic tannery wastewater in 0.10 mol L^{-1} Na_2SO_4.

Tabla 2. Eliminación de TOC y consumo energético obtenido tras 4 h de oxidación electroquímica de un agua sintética procedente del curtido de pieles en Na_2SO_4 0.1M.

Electrolysis condition	TOC removal (%)	Energy consumption per removed TOC ($kWhg^{-1}$)
Ti/SnO_2–Sb–Ir, 25$mAcm^{-2}$	2.1	2.55
Ti/SnO_2–Sb, 25$mAcm^{-2}$	56.1	0.10
Si/BDD, 25$mAcm^{-2}$	79.1	0.08
Si/BDD, 100$mAcm^{-2}$	98.3	0.55

5. Conclusions

Electrochemical treatment of wastewaters have undergone rapid development due to the appearance of a new material: boron doped diamond films. These BDD electrodes are attractive as anodic material due to their high physical, chemical and electrochemical stability and mainly in the wastewater treatment, due to their high overpotential for water oxidation-reduction processes. These properties confirm these BDD materials as one of the most promising electrode material for the treatment of industrial pollutants in water.

The good agreement between the experimental data and the theoretical model indicates that these electrodes present the maximum efficiency in pollutant removal, just limited by diffusion-controlled electrochemical kinetics. In the case of benzoic acid on the reaction proceeds by electrogenerated intermediates (hydroxyl radicals) on BDD and it is a fast reaction. The electrochemical treatment of more complex systems (synthetic tannery wastewater) indicates that Si/BDD electrode exhibits the best performance for the removal of total phenols, COD, TOC, and colour.

6. References

[1] H.Davy, *Phil. Trans. R. Soc. Lond.* **1808**, *98*, 1.

[2] R.L.McCreery, *Chemical Reviews* **2008**, *108*, 2646.

[3] I.Svancara, K.Vytras, K.Kalcher, A.Walcarius, J.Wang, *Electroanalysis* **2009**, *21*, 7.

[4] Y.V.Pleskov, *Uspekhi Khimii* **1999**, *68*, 416.

[5] P.L.Hagans, P.M.Natishan, B.R.Stoner, W.E.O'Grady, *Journal of the Electrochemical Society* **2001**, *148*, E298-E301.

[6] A.E.Fischer, M.A.Lowe, G.M.Swain, *Journal of the Electrochemical Society* **2007**, *154*, K61-K67.

[7] M.C.Granger, M.Witek, J.S.Xu, J.Wang, M.Hupert, A.Hanks, M.D.Koppang, J.E.Butler, G.Lucazeau, M.Mermoux, J.W.Strojek, G.M.Swain, *Analytical Chemistry* **2000**, *72*, 3793.

[8] J.Wang, G.M.Swain, *Journal of the Electrochemical Society* **2003**, *150*, E24-E32.

[9] F.Montilla, E.Morallon, I.Duo, C.Comninellis, J.L.Vazquez, *Electrochimica Acta* **2003**, *48*, 3891.

[10] M.Panizza, P.A.Michaud, G.Cerisola, C.Comninellis, *Journal of Electroanalytical Chemistry* **2001**, *507*, 206.

[11] O.Simond, V.Schaller, C.Comninellis, *Electrochimica Acta* **1997**, *42*, 2009.

[12] F.Montilla, P.A.Michaud, E.Morallon, J.L.Vazquez, C.Comninellis, *Electrochimica Acta* **2002**, *47*, 3509.

[13] C.R.Costa, F.Montilla, E.Morallon, P.Olivi, *Electrochimica Acta* **2009**, *54*, 7048.

[14] C.R.Costa, F.Montilla, E.Morallon, P.Olivia, *Journal of Hazardous Materials* **2010**, *180*, 429.

El carbón activado como promotor de especies altamente oxidantes en su interacción con la radiación gamma

Activated carbon as promoter of highly oxidant species in its interaction with gamma radiation

I. Velo-Gala, J. J. López-Peñalver, M. Sánchez-Polo, J. Rivera-Utrilla

Department of Inorganic Chemistry, Faculty of Science, University of Granada, 18071 Granada, Spain

Corresponding author: mansanch@ugr.es

Resúmen

El objetivo de este estudio fue analizar la influencia de la presencia de carbón activado en la degradación del medio de contraste triyodado diatrizoato (DTZ) mediante la utilización simultánea de radiación gamma y carbón activado. Cuatro carbones activados comerciales (Ceca, Witco, Sorbo y Merck) con diferentes características químicas y texturales fueron utilizados para este propósito. El porcentaje de degradación de DTZ obtenido fue considerablemente mayor con el sistema radiación gamma/carbón activado (GM/CA) que con la radiolisis en ausencia de carbón activado, y este sistema dependían de la cantidad específica de carbón activo empleado. En primer lugar, hemos optimizado la cantidad de carbón activado necesario para maximizar la cantidad de DTZ eliminado por el sistema GM/CA (0,06 g). Las constantes de velocidad de degradación fueron mayores con el sistema GM/AC que con sólo radiolisis, lo que evidencia un efecto sinérgico que favorece la eliminación de los contaminantes. Este efecto sinérgico es independiente de las características texturales del carbón activado, pero no de sus características químicas, observándose una mayor actividad sinérgica de los carbones con un contenido superficial más alto de oxígeno, concretamente de grupos quinona. Para que el efecto sinérgico tenga lugar se requiere la presencia de interacciones electrostáticas adsorbente-adsorbato.

Abstract

The objective of this study was to analyse the influence of the presence of activated carbon on the degradation of the triiodinated contrast medium diatrizoate (DTZ) by the simultaneous use of gamma radiation and activated carbon. Four commercial activated carbons (Ceca, Witco, Sorbo and Merck) with different textural and chemical characteristics were used for this purpose. The percentage DTZ removal obtained was considerably higher with the gamma radiation/activated carbon (GM/AC) system than with radiolysis in the absence of activated carbon, and it depended on the specific activated carbon employed. The amount of activated carbon required to maximize the amount of DTZ removed by the GM/AC system (0.06 g) was optimized. The degradation rate constants were higher with the GM/AC system than with radiolysis alone, evidencing a synergic effect that favours pollutant removal. This synergic effect is independent of the textural but not the chemical characteristics of the activated carbon, observing a higher synergic activity for activated carbons with greater surface oxygen content, specifically quinone groups. It is also highlighted that the synergic effect of the activated carbon requires adsorbent–adsorbate electrostatic interactions, and this effect is absent when these interactions are hindered.

1. Introducción

Actualmente, el uso de carbón activado (CA) en la eliminación de compuestos orgánicos e inorgánicos de las aguas es considerado como una de las mejores alternativas disponibles en el tratamiento terciario de los efluentes en las estaciones depuradoras de aguas residuales urbanas. La cantidad y tipología de contaminantes que pueden eliminarse mediante CAs es muy amplia y ello gracias a las propiedades fisicoquímicas de su superficie. Estas cualidades de los CAs pueden modificarse con la utilización de diferentes métodos de activación, por lo que pueden elaborarse carbones conforme a objetivos de eliminación específicos. Esta versatilidad en su aplicación aumenta si se considera el hecho de su utilización combinada con otros procesos físicos y químicos, como son los procesos de oxidación avanzada o su aplicación en catálisis, lo que supone la existencia de innumerables posibilidades para el tratamiento de todo tipo de contaminantes. Es en este contexto donde cobra especial interés la aplicación del CA como agente potenciador de la efectividad de los sistemas de tratamiento convencionales. Concretamente en este trabajo se analiza el comportamiento del carbón activado en su interacción con la radiación gamma y su efectividad en la eliminación de los contaminantes presentes en las aguas. Para llevar a cabo este estudio se seleccionó el diatrizoato sódico como compuesto modelo (DTZ).

Tras la realización de los estudios pertinentes sobre la eliminación del DTZ en procesos de adsorción en CA y su degradación por radiolisis, se propuso la utilización simultánea de ambos sistemas para lograr una opción de tratamiento que elimine del medio acuático tanto el contaminante tóxico original como los productos de degradación. En algunos casos, la vía oxidante es muy lenta, siendo más favorable el empleo de radicales reductores como es el caso de los electrones solvatados (e^-_{aq}) o los radicales hidrógeno ($H^\bullet$); de aquí que se plantee el tratamiento de las aguas con tecnologías que permitan generar a la vez especies oxidantes y reductoras como es el caso de las radiaciones ionizantes, constituyendo una alternativa a considerar en el tratamiento de contaminantes resistentes a las tecnología usuales. Sin embargo, el papel que desempeña la presencia de catalizadores en este proceso y, concretamente, el CA durante la irradiación de aguas contaminadas es un área de investigación totalmente inexplorada en la actualidad. El uso del CA en el proceso radiolítico podría inducir un efecto sinérgico que potenciaría la degradación del compuesto, permitiendo la obtención de resultados que van más allá de la suma de los porcentajes de degradación que cabría esperar, debidos al efecto combinado de los radicales oxidantes y reductores procedentes de la radiolisis

y los grupos oxidantes del carbón, junto con su capacidad de adsorción. Además, la recuperación del CA utilizado es posible mediante sencillos sistemas de decantación, siendo esto de mayor dificultad en los casos en los que se aplican catalizadores como el dióxido de titanio. Por todo ello, el uso de CA en presencia de fuentes de energía constituye un nuevo procedimiento que podría aplicarse en los actuales sistemas de tratamiento de efluentes que utilizan radiolisis, con objeto de lograr su optimización.

En este trabajo, por lo tanto, se profundiza en el estudio de la acción que tiene la adición de diferentes CAs en la degradación radiolítica de los contaminantes, empleando como compuesto modelo el DTZ. Para ello, se abordarán los siguientes aspectos: i) la cinética del proceso radiolítico en presencia de CAs con diferentes propiedades texturales y químicas; ii) los mecanismos implicados en el proceso de eliminación de DTZ mediante el uso combinado de CAs y radiación gamma, y iii) la influencia de las características físicas y químicas de los carbones en el rendimiento del proceso conjunto. La parte experimental de este trabajo se ha publicado en artículos previos [1,2,3].

2. Resultados y discusión

2.1. Influencia de la dosis de carbón activado en la radiolisis de DTZ

El tratamiento radiolítico del DTZ en presencia de CA es un proceso complejo en el cual el descenso en la concentración del DTZ se puede describir como la suma de tres procesos: a) el proceso radiolítico; b) el proceso de adsorción; y c) el efecto sinérgico que produce la presencia del CA. Este efecto sinérgico puede tener signo positivo, si favorece la degradación del DTZ, ser igual a cero, si no influye en el proceso, o bien negativo, si para una misma dosis la cantidad de DTZ presente en el medio después del tratamiento es mayor que cuando se realiza el tratamiento en ausencia de CA. La constante de velocidad de eliminación de DTZ observada (K_{ob}) se puede expresar como la suma de tres variables (Ecuación 1):

$$k_{ob} = k_{Rad} + k_{Ad} + k_{SE} \qquad (1)$$

Donde k_{Rad} es la constante de velocidad de eliminación del DTZ debida al proceso radiolítico (Gy^{-1}), k_{Ad} es la constante de velocidad que rige el proceso de adsorción (Gy^{-1}) y k_{SE} expresa la constante de velocidad debida al efecto sinérgico. Por lo tanto, para poder calcular el valor de k_{SE} es necesario determinar la contribución del proceso de radiolisis y del proceso de adsorción, ambos por separado.

Para cuantificar la influencia de la adsorción y de la radiolisis de DTZ se obtuvieron las cinéticas de adsorción y del proceso radiolítico, por separado, en las mismas condiciones en las que se obtuvo la cinética de eliminación del DTZ por radiolisis en presencia de CA.

El estudio de la influencia de la adición del CA en el proceso de eliminación del DTZ mediante el uso de radiolisis conlleva determinar la cantidad óptima de CA a adicionar. Así, se obtuvo la superficie de respuesta que permite determinar la variación del porcentaje de DTZ degradado en función de la dosis de radiación absorbida y de la cantidad de carbón presente en el medio. Para ello, se empleó la modelización denominada distancia ponderada por mínimos cuadrado (Distance-Weighted Least Squares Fitting) que permite obtener una superficie de respuesta que pasa por todos y cada uno de los datos experimentales. La superficie respuesta obtenida se muestra en Figura 1A, observándose que el porcentaje de eliminación máximo se obtiene para el intervalo de masa de CA de 0.06-0.08 g.

2.2. Influencia del tipo de carbón activado en la radiolisis de DTZ

Una vez determinada la cantidad óptima de CA, se obtuvieron las cinéticas de eliminación de DTZ en presencia de cuatro carbones comerciales con características químicas y texturales diferentes: Witco (W), Ceca (C), Merck (M) y Sorbo (S) [1, 2].

En la Tabla 1 se muestran los resultados de eliminación de DTZ obtenidos para los cuatro carbones, observándose que el porcentaje de DTZ eliminado al final del proceso, para una dosis de 600 Gy, es muy superior cuando la radiolisis se lleva a cabo en presencia de los CAs (Experimentos Núm. 2-5, Tabla 1), frente al obtenido en su ausencia (Experimento

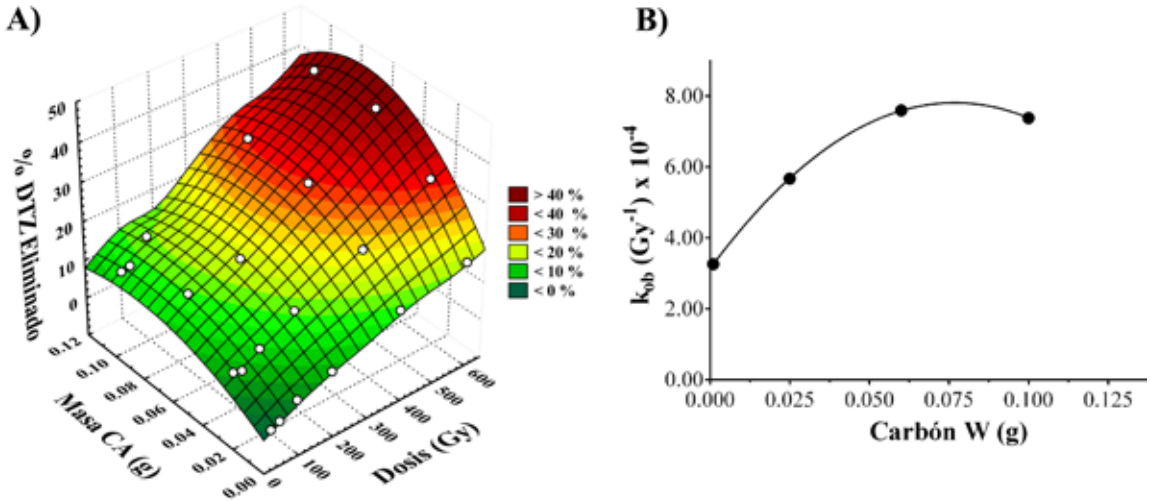

Figura 1. A), Superficie de respuesta obtenida mediante la modelización "*Distancia ponderada por mínimos cuadrados*". B), Variación de la constante de degradación en función de la masa de carbón W presente en el medio.

Figure 1. A), Response surface obtained by modelling *Distance-Weighted Least Squares Fitting*. B), Variation in the DTZ degraded rate constant as a function of the mass of carbon W in the medium.

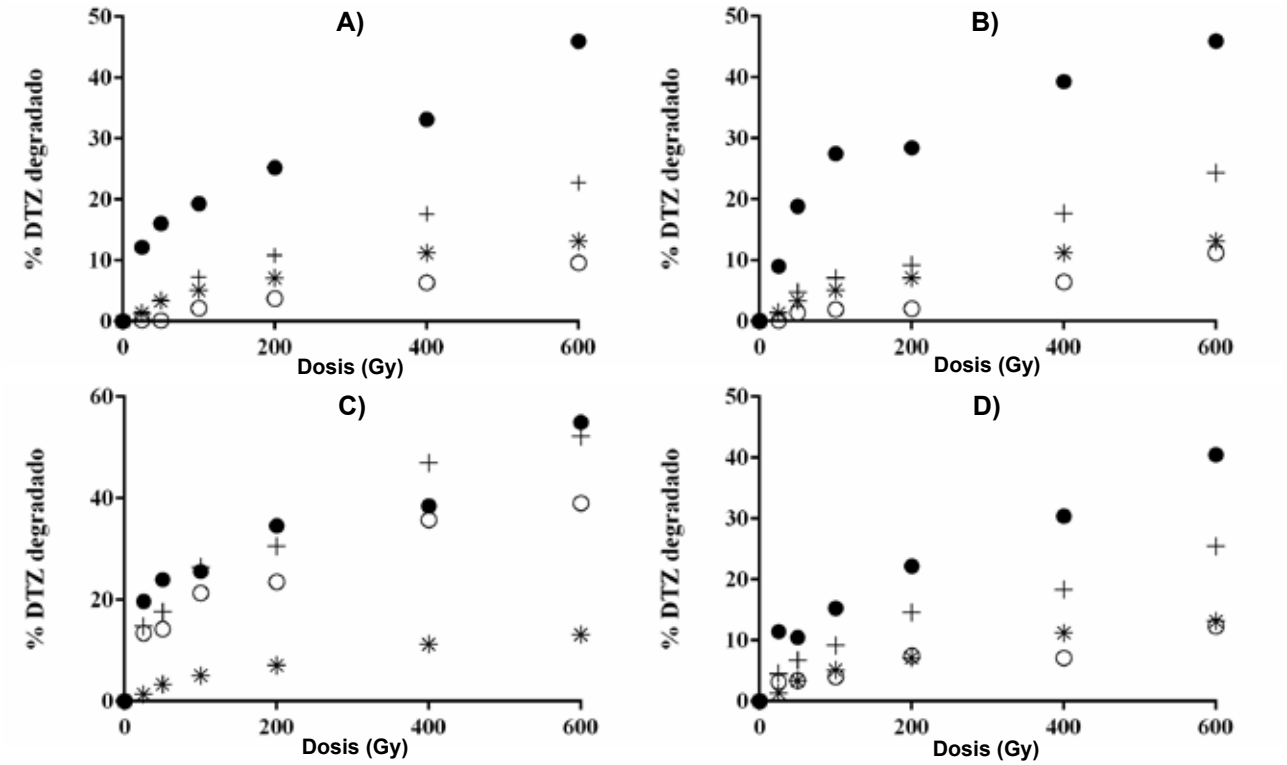

Figura 2. Porcentajes de eliminación del DTZ mediante cuatro sistemas: (✳) radiolisis sin CA; (●) radiolisis en presencia de CA; (○) adsorción del DTZ sobre CA; y (+) efecto teórico sumatorio de los la adsorción más radiolisis. A) Serie carbón C; B) serie carbón M; C) serie carbón S; D) serie carbón W. $[DTZ_0]$ = 1000 mg L^{-1}. P_{CA} = 0.06 g de CA. T = 298 K. pH = 6.5. Tasa de Dosis = 1.66 Gy min^{-1}.

Figure 2. Percentage DTZ removal with four systems: (✳) radiolysis without AC; (●) radiolysis in the presence of AC; (○) DTZ adsorption on AC; and (+) theoretical sum effect of adsorption plus radiolysis. A) carbon C series; B) carbon M series; C) carbon S series; D) carbon W series. $[DTZ_0]$ = 1000 mg L^{-1}. Amount of AC = 0.06 g. T = 298 K. pH = 6.5. Dose Rate = 1.66 Gy min^{-1}.

Núm. 1, Tabla 1). Además, el comportamiento de los cuatro CAs difiere el uno del otro, alcanzándose el valor máximo de eliminación para el carbón S. Los valores de las constantes de velocidad de eliminación observada, k_{ob}, determinados, junto con los porcentajes de eliminación, se muestran en la Tabla 1.

Los resultados obtenidos muestran que la radiolisis del DTZ en presencia de CAs mejora el proceso de eliminación del DTZ en los cuatro carbones comerciales considerados, como demuestran los altos valores de las constantes de reacción y los porcentajes de degradación obtenidos, frente a los determinados para el proceso en ausencia de CA (Experimento Núm. 1). Sin embargo, hay que tener en cuenta el proceso de adsorción del DTZ sobre el CA para valorar si la mejora observada es únicamente debida a la suma del proceso de adsorción sobre el CA más la degradación por la radiación gamma o si, por el contrario, la presencia de CA potencia la degradación y, por tanto, se obtienen resultados superiores al esperado por el efecto de adición de ambos procesos. Por ello, se obtuvieron las cinéticas de adsorción del DTZ para los cuatro CAs estudiados, en las mismas condiciones experimentales en las que se llevó a cabo el proceso radiolítico en presencia del CA. Los resultados obtenidos se

Tabla 1. Condiciones experimentales y parámetros cinéticos obtenidos en la degradación del DTZ mediante radiación gamma en presencia y ausencia de CA. $[DTZ]_0$ = 1000 mg L^{-1}. P_{CA} = 0.06 g de CA. Tasa de Dosis = 1.66 Gy min^{-1}. pH = 6.5. T = 298 K.

Table 1. Experimental conditions and kinetic parameters for DTZ removal by gamma radiation in the presence and absence of activated carbons. [DTZ]0 = 1000 mg L-1. Amount of AC = 0.06 g. Dose Rate = 1.66 Gy min-1. pH = 6.5. T = 298 K.

Nº. Exp.	Carbón	pH	% Degradado	$k_{ob}x10^4$ (Gy^{-1})
1	---	6.5	13.15	1.8 ± 0.1
2	C	6.5	45.98	8.2 ± 0.2
3	M	6.5	45.93	7.4 ± 0.2
4	S	6.5	54.97	9.9± 0.4
5	W	6.5	40.49	6.8 ± 0.2

Tabla 2. Condiciones experimentales y parámetros cinéticos obtenidos para la adsorción del DTZ sobre los CAs. $[DTZ]_0$ = 1000 mg L^{-1}. P_{CA} = 0.06 g de CA. Tasa de Dosis = 1.66 Gy min^{-1}. pH = 6.5. T = 298 K.

Table 2. Experimental conditions and kinetic parameters obtained for DTZ adsorption on activated carbons. $[DTZ]_0$ = 1000 mg L^{-1}. Amount of AC = 0.06 g. Dose Rate = 1.66 Gy min^{-1}. pH = 6.5. T = 298 K.

Nº. Exp.	Carbón	pH	% DTZ Adsorbido	$K_{Ad}x10^6$ (s^{-1})	$k_{Ad}x10^4$ (Gy^{-1})	$k_{SE}x10^4$ (Gy^{-1})
6	C	6.5	9.60	3.7 ± 0.1	1.56 ± 0.06	4.8 ± 0.4
7	M	6.5	11.17	4.6 ± 0.4	1.9 ± 0.1	3.7 ± 0.5
8	S	6.5	39.02	14.7 ± 0.7	6.13± 0.02	1.9 ± 0.8
9	W	6.5	12.32	6.5 ± 0.6	2.7 ± 0.2	2.3 ± 0.6

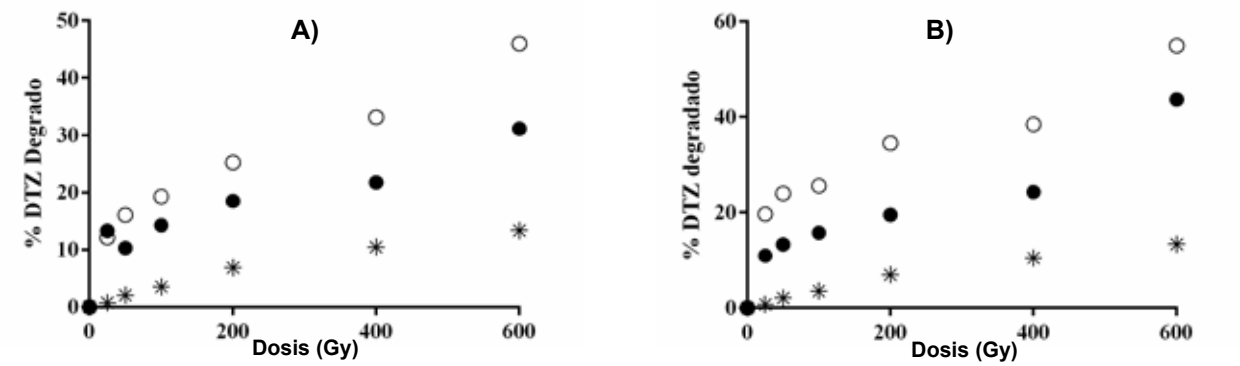

Figura 3. Efecto de los carbones saturados en la degradación del DTZ por radiolisis: (✳), sin CA; (●), con CA saturado; (○), con CA sin saturar. A) Serie del carbón C; B) serie del carbón S. $[DTZ_0]$ = 1000 mg L^{-1}. P_{CA} = 0.06 g de CA. T = 298 K. pH = 6.5. Tasa de Dosis = 1.66 Gy min^{-1}.

Figure 3. Effect of saturated carbons on DTZ degradation by radiolysis: (✳), without AC; (●), with saturated AC; (○), with non-saturated AC. A) carbon C series; B) carbon S series. $[DTZ_0]$ = 1000 mg L^{-1}. Amount of AC = 0.06 g. T = 298 K. pH = 6.5. Dose Rate = 1.66 Gy min^{-1}.

muestran en la Tabla 2. Una vez determinado el valor de k_{Ad}, se puede determinar el valor de k_{SE}, siendo la contribución de k_{SE} al valor de k_{ob} de un 58.26%, 49,57%, 19.09% y 33.29% para los carbones C, M, S y W, respectivamente. Los resultados obtenidos muestran que en todos los casos se produce una sinergia positiva y que ésta aumenta en el sentido S<W<M<C.

En la Figura 2 se muestra, para cada uno de los carbones activados considerados, la variación del porcentaje del DTZ eliminado: i) en el proceso de radiolisis; ii) en el proceso de adsorción); iii) la suma de los procesos de adsorción y radiolisis por separado (i + ii); y iv) en el proceso de radiolisis en presencia de CA. Como puede observarse, los resultados muestran la existencia de un efecto sinérgico de la radiolisis en presencia de CA, siendo la diferencia entre el proceso radiolítico en presencia de CA y la suma de los procesos de radiolisis del DTZ en ausencia de CA y el proceso de adsorción, más acusada en el caso de los carbones C y M. Por el contrario, como se observa en el caso del carbón S, cuando la velocidad de adsorción del DTZ sobre el CA es elevada el efecto sinérgico determinado es menor.

Al objeto de evaluar el efecto sinérgico en ausencia del proceso de adsorción, se llevaron a cabo experimentos de radiolisis del DTZ en presencia de CA saturado con DTZ. Los resultados obtenidos se recogen en la Tabla 3. En la Figura 3 se muestra gráficamente la comparación del proceso radiolítico usando carbones saturados con DTZ y sin saturar.

Los valores de k_{SE} determinados para los CAs saturados revelan que el efecto sinérgico se mantiene en los carbones saturados y, además, dichos valores muestran la capacidad real del CA para potenciar la degradación. Así, en el caso del carbón S, el cual presentaba una componente adsortiva elevada (Tabla 2), su efecto sinérgico se multiplica por tres pasando de (1.9 ± 0.8)x10^{-4} a (6.1 ± 0.8)x10^{-4} Gy^{-1}. Por lo tanto, cuando los CAs presentan cinéticas de adsorción rápidas, disminuye la contribución del efecto sinérgico al proceso global de la radiolisis en presencia de carbón.

Al comparar los resultados obtenidos (Tabla 2) con las características químicas y texturales de los CAs [1, 2], se observa que las características texturales no son determinantes en el efecto sinérgico obtenido ya que, por ejemplo, el carbón M que es el que posee una mayor área superficial (S_{BET}=1493 m^2 g^{-1}) presenta una k_{SE} = (3.7 ± 0.5)x10^{-4} Gy^{-1}, valor inferior al que presenta el carbón C (k_{SE} = (4.8 ± 0.4)x10^{-4} Gy^{-1}) que posee un área superficial S_{BET}=1294 m^2 g^{-1}. Por otra parte, el resto de parámetros texturales determinados (V_T, D_P y S_{Ext}) tampoco guardan una estrecha relación con la variación observada en el valor de k_{SE}. Por ello, el carácter potenciador en la degradación del DTZ que presentan estos materiales, mediante el uso de radiación gamma, podría estar relacionado con sus propiedades químicas. Si se consideran los resultados obtenidos para los CAs saturados, se observa que el CA con un mayor contenido en oxígeno superficial, carbón S, es el que posee un mayor efecto sinérgico. Para explicar este comportamiento, se debe considerar que la radiación gamma interacciona tanto con el CA presente como con la molécula de agua. Al poseer el carbono un número atómico bajo y tener la radiación incidente una energía de 0.6617 MeV, el efecto predominante en la interacción de la radiación con el CA es el efecto Compton. De esta forma, el mecanismo de interacción predominante es la ionización, en la cual los fotones incidentes interaccionan con los electrones de los orbitales de los átomos superficiales y producen iones positivos y electrones libres. Por lo tanto, los átomos de carbono situados en la superficie contribuyen a aumentar los electrones libres presentes en el medio, favoreciendo la degradación (vía reducción) del DTZ, lo que

Tabla 3. Parámetros cinéticos obtenidos para la radiolisis del DTZ en presencia de los carbones activados C y S saturados. $[DTZ]_0$ = 1000 mg L^{-1}. P_{CA} = 0.06 g de CA. Tasa de Dosis = 1.66 Gy min^{-1}. pH = 6.5. T = 298 K.

Table 3. Kinetic parameters obtained for DTZ radiolysis in the presence of saturated activated carbons C and S. $[DTZ]_0$ = 1000 mg L^{-1}. Amount of CA = 0.06 g. Dose Rate= 1.66 Gy min^{-1}. pH = 6.5. T = 298 K.

Nº. Exp.	Carbón	pH	% Degradado	$k_{Rad}x10^5$ (Gy^{-1})	$k_{ob}x10^4$ (Gy^{-1})	$k_{SE}x10^4$ (Gy^{-1})
10	-	6.5	13.37	17.9 ± 0.8	-	-
11	C_{SAT}	6.5	31.16	-	4.6 ± 0.3	2.8 ± 0.5
12	S_{SAT}	6.5	43.66	-	7.9 ± 0.4	6.1 ± 0.8

justifica el efecto sinérgico observado para los cuatro CAs. Además, el oxígeno quimisorbido presente en los cuatro carbones puede atrapar electrones dando lugar a la formación del anión superóxido [1, 2]. El anión superóxido formado puede interaccionar directamente con el DTZ, o bien formar más radicales (Reacción 2). Todo ello contribuye a favorecer la degradación del DTZ, ya que se favorece la generación de una nueva especie oxidante en el medio. Ambos efectos explican el efecto sinérgico observado para la radiolisis del DTZ en presencia de CAs.

$$O^{\bullet}_2{}^{-} + H_3O^+ \rightarrow HO^{\bullet} + H_2O + \tfrac{1}{2}\, O_2 \qquad (2)$$

$$k = 4.5\times10^{10}\ M^{-1}\ s^{-1}$$

Además, la radiación gamma incidente también interacciona con las moléculas de agua dando lugar a los procesos esquematizados en las Reacciones 3 a 7:

$$H_2O \xrightarrow{\text{Radiación } \gamma} H_2O^{\bullet+} + e^- \qquad (3)$$

$$H_2O \xrightarrow{\text{Radiación } \gamma} H_2O^* \qquad (4)$$

$$H_2O^{\bullet+} \rightarrow HO^{\bullet} + H^+ \qquad (5)$$

$$e^- + nH_2O \rightarrow e^-_{aq} \qquad (6)$$

$$H_2O^* \rightarrow HO^{\bullet} + H^{\bullet} \qquad (7)$$

Mediante las reacciones anteriores se forman los radicales del proceso radiolítico que pueden interaccionar tanto con el DTZ como con el CA presentes en el medio, así como dar lugar a reacciones de recombinación radicalaria (Reacciones 8-11).

$$HO^{\bullet} + H^{\bullet} \rightarrow H_2O \qquad k = 7.0\times10^{9}\ M^{-1}\ s^{-1} \qquad (8)$$

$$H^{\bullet} + H^{\bullet} \rightarrow H_2 \qquad k = 7.75\times10^{9}\ M^{-1}\ s^{-1} \qquad (9)$$

$$e^-_{aq} + H^{\bullet} + H_2O \rightarrow H_2 + HO^- \qquad k = 2.5\times10^{10}\ M^{-1}\ s^{-1} \qquad (10)$$

$$HO^{\bullet} + e^-_{aq} \rightarrow HO^- \qquad k = 3.0\times10^{10}\ M^{-1}\ s^{-1} \qquad (11)$$

Los grupos oxigenados superficiales presentes en los CAs, y en particular los grupos quinona, son capaces de estabilizar radicales en su superficie [1]. Si consideramos los resultados obtenidos para los carbones saturados, donde ya no influye el proceso de adsorción, se observa que el valor más elevado de k_{SE} se obtiene para el carbón Sorbo, carbón que presenta un mayor porcentaje de grupos quinonas [1, 2]. Este resultado sugiere que los radicales formados durante la radiolisis podrían interaccionar con la superficie de carbón para dar lugar a zonas de una alta reactividad debido a los radicales así estabilizados. Este mecanismo será tanto más influyente cuanto mayor sea el contenido en quinonas, lo que justifica que el k_{SE} más elevado se haya obtenido para el carbón S.

3. Conclusiones

Los resultados obtenidos muestran que el sistema radiolisis/CA aumenta la eficiencia en la eliminación del DTZ, en comparación con el tratamiento en ausencia de CA. Además, el efecto sinérgico observado es independiente de las propiedades texturales de carbón, no así de su naturaleza química superficial.

El contenido en oxígeno de los CAs influye de forma determinante en la extensión del efecto sinérgico observado. Así, el carbón C, material que posee un mayor contiendo en oxígeno, es el que muestra un mayor efecto sinérgico en el proceso de radiolisis.

Los radicales formados durante la radiolisis pueden interaccionar con la superficie de carbón para dar lugar a zonas de una alta reactividad debido a la elevada concentración de radicales estabilizados por los grupos quinona presentes en la superficie del CA. Este mecanismo será tanto más influyente cuanto mayor sea el contenido en quinonas.

La presencia de oxígeno quimisorbido en la superficie del carbón influye en el proceso de eliminación del contaminante, ya que contribuye a la formación del anión superóxido que puede interaccionar con el DTZ y/o formar nuevas especies oxidantes que contribuyen a la degradación del contaminante.

4. Bibliografía

[1] Velo-Gala I, López-Peñalver J J, Sánchez-Polo M, Rivera-Utrilla J. Role of activated carbon on micropollutans degradation by ionizing radiation. Carbon, Volume 67, February 2014, Pages 288-299

[2] Velo-Gala I, López-Peñalver J J, Sánchez-Polo M, Rivera-Utrilla J. Surface modifications of activated carbon by gamma irradiation. Carbon, Volume 67, February 2014, Pages 236-249

[3] Velo-Gala I, López-Peñalver J J, Sánchez-Polo M, Rivera-Utrilla J. Degradation of X-ray contrast media diatrizoate in different water matrices by gamma irradiation. J. Chem. Techno. Biotechnol., Volume 88, January 2013, Pages 1336–1343

Carbon materials as catalysts for the ozonation of organic pollutants in water

Materiales de carbón como catalizadores para la ozonización de contaminantes orgánicos en agua

M. F. R. Pereira, A. G. Gonçalves, J. J.M. Órfão*

Laboratório de Catálise e Materiais (LCM), Laboratório Associado LSRE/LCM, Departamento de Engenharia Química, Faculdade de Engenharia, Universidade do Porto, Rua Dr. Roberto Frias, 4200-465 Porto, Portugal

**Corresponding author: fpereira@fe.up.pt*

Abstract

A brief overview about the use of carbon materials as metal free ozonation catalysts is presented. Carbon materials (activated carbons, carbon xerogels, carbon nanofibers and carbon nanotubes) have been shown to be active catalysts in the ozonation of a wide range of organic pollutants. Carbon materials with surface basic properties (i.e. high electron density) and with large pores are the most promising for this process.

Resumen

En el presente trabajo se resume brevemente el uso de materiales de carbón como catalizadores libres de metales en el proceso de ozonización. Los materiales de carbón (carbones activados, xerogeles de carbón, nanofibras y nanotubos de carbono) han mostrado ser catalizadores activos para una gran variedad de contaminantes orgánicos en dicho proceso, siendo los más adecuados aquellos con propiedades superficiales básicas (alta densidad electrónica) y con mayor tamaño de poros.

1. Ozone reactivity in water

The high reactivity of ozone can be attributed to the electronic configuration of the molecule. The two extreme forms of resonance structures of ozone molecule are illustrated in Figure 1. The absence of electrons in one of the terminal oxygen atoms in some of the resonance structures confirms the electrophilic nature of ozone. Conversely, the excess negative charge present in some other oxygen atom imparts a nucleophilic character to the molecule [1, 2].

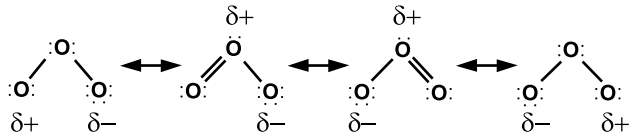

Figure 1. Resonance structures of the ozone molecule. Adapted from [1].

Figura 1. Estructuras de resonancia de la molécula de ozono [1]. Adaptado de [1].

Ozone has one of the highest standard redox potential (2.07 V), only lower than those of fluorine (3.06 V), hydroxyl radical (2.80 V) and atomic oxygen (2.42 V). Because of its high standard redox potential, the ozone molecule has a high capacity to react with numerous compounds by means of redox reactions. Some of these reactions occur by explicit electron transfer, while most of them occur by oxygen transfer from the ozone molecule to the other reactant [1, 2].

The stability of ozone in water largely depends on the water matrix, especially its pH, temperature, chemical composition (such as, the presence of natural organic matter (NOM) and bicarbonate/carbonate ions) [3].

Ozone reactions in water can be classified as direct and indirect reactions, as presented in Figure 2. Direct reactions occur between ozone molecules and other chemical species (M), while indirect reactions are those between the $HO^{\bullet}$ radicals (formed from the decomposition of ozone or from other direct ozone reactions) and compounds present in water. In contrast to other conventional oxidant species, hydroxyl radicals are capable to completely oxidise (i.e. mineralise) even the less reactive pollutants. They react non-selectively with organic compounds, mainly by means of electrophilic addition to unsaturated bonds, addition to aromatic rings, abstraction of hydrogen or by electron transfer. The rate constants of most reactions between $HO^{\bullet}$ and organic species are usually in the order of 10^6 -10^9 M^{-1} s^{-1} [4]. Mineralisation of end products generally results in inorganic carbon, water and inorganic ions.

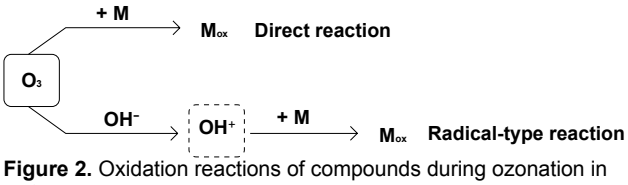

Figure 2. Oxidation reactions of compounds during ozonation in water.

Figura 2. Reacciones de oxidación de compuestos durante la ozonización en agua.

The spontaneous decomposition of ozone in aqueous solution occurs through a series of steps. Since the first model proposed by Weiss in 1935 [5], numerous studies have been developed to clarify the mechanism of decomposition of ozone in water. Presently, the mechanism proposed by Staehelin and Hoigné [6] is generally accepted for the decomposition of dissolved ozone, but alternative reaction steps have been proposed by other authors. A review of the proposed mechanisms is presented in [2]. Briefly, the mechanism for the decomposition of dissolved ozone is described below [7]:

Initiation:
$$O_3 + H_2O \rightarrow 2HO^{\bullet} + O_2 \quad (1)$$
$$O_3 + HO^- \rightarrow O_2^{\bullet -} + HO_2^{\bullet} \quad (2)$$

Propagation:
$$O_3 + HO^{\bullet} \rightarrow O_2 + HO_2^{\bullet} \quad (3)$$
$$O_3 + HO_2^{\bullet} \rightarrow 2O_2 + HO^{\bullet} \quad (4)$$

Termination:
$$2HO_2^{\bullet} \rightarrow O_2 + H_2O_2 \quad (5)$$

The initiation steps of the ozone decomposition chain mechanism consist in reaction of ozone with water (reaction 1) and hydroxide ions (reaction 2) originating hydroxyl radicals. Nevertheless, the initiation of ozone decomposition in aqueous solution can be artificially accelerated by increasing the pH or by the addition of UV radiation, hydrogen peroxide, reduced metal ions or heterogeneous catalysts, leading to an Advanced

Oxidation Process (AOP) [8]. The contribution of these two steps for ozone decomposition depends strongly on the pH of the solution and on the nature of the substances present in water. Normally, under acidic conditions (pH < 4) the direct pathway rules, whereas for pH > 10 mainly the radical pathway is present. Under neutral conditions, both pathways can be important [9].

The ozone decomposition chain can be terminated when hydroxyl radicals react with inhibitors, which are compounds capable of consuming $HO^{\bullet}$ radicals without regenerating the superoxide radical. The more common inhibitors include tertiary alcohols (e.g. *tert*-butanol), and carbonate and bicarbonate ions. These are also called hydroxyl radical scavengers, because their presence limits or inhibits the action of these radicals on the target compounds. *Tert*-butanol is a well-known radical scavenger, as it reacts with $HO^{\bullet}$ at a rate constant of 5×10^8 M^{-1} s^{-1} [10], which is in the range of the rate constants of reactions between $HO^{\bullet}$ and organic compounds.

2. Catalytic ozonation for the degradation of organic compounds

Catalytic ozonation is an AOP for contaminants removal from drinking water and wastewater. Presently, the application of catalytic ozonation is mainly limited to laboratory use. However, due to successful results, further investigation is to be carried out. The target pollutants are organic compounds refractory to biological treatments, such as pesticides, endocrine disrupting compounds (EDCs), pharmaceuticals, and personal care products (PPCPs) and textile dyes. The main weakness of non-catalytic ozonation is related to by-products formation and their future damage in the environment. In contrast, in catalytic ozonation, the problem of toxic by-products formation can be solved by the development of active catalysts capable to promote their mineralisation.

In water treatment, the high reactivity of ozone and the active surfaces of some materials can be used to increase the ozonation efficiency. In this way, several research groups have been focussed on the combined application of ozone and solid catalysts, and consequently numerous papers have been published since the mid 1990s. The most common catalysts proposed for the process of heterogeneous catalytic ozonation are metal oxides such as MnO_2, TiO_2, Al_2O_3, ZnO and supported metal oxides (TiO_2/Al_2O_3, Fe_2O_3/Al_2O_3, Co_3O_4/Al_2O_3, MnO_2/TiO_2) [11]. Transition and noble metals supported on several oxides (Cu-Al_2O_3, Cu-TiO_2, Ru-CeO_2, Co-Al_2O_3) have also been investigated [11, 12]. Activated carbon by itself [13-15], carbon xerogels [16], carbon nanotubes [17], metal oxides supported on activated carbon [18], metal-doped carbon aerogels [19] and platinum supported on carbon nanotubes [20] have also been tested in the ozonation of organic compounds.

The activity of such materials is frequently associated with their ability to catalytically decompose ozone leading to the formation of $HO^{\bullet}$ radicals. The efficiency of the catalytic ozonation process depends, to a great extent, on the catalyst and its surface properties, as well as on the pH of the solution, which influences the properties of surface active sites and ozone decomposition reactions in the aqueous phase. The huge diversity of solid catalyst types, the variety of the surface properties, and the interactions between catalyst, ozone and organic molecules, make difficult the generalisation of the mechanisms involved. In the following sections a more detailed discussion on the ozonation catalysed by carbon materials is presented.

3. Carbon as catalyst for ozonation

3.1 Catalytic decomposition of ozone in water

Concerning wastewater treatment, the instability of ozone molecule is an advantage, as the formation of $HO^{\bullet}$ radicals transforms ozonation into an advanced oxidation process [2], enhancing its efficiency for the degradation of organic pollutants.

Carbon materials by themselves were found to be catalysts for the decomposition of O_3 in water. The pioneer work on this subject was carried out by Jans and Hoigné [21]. Suspensions of activated carbon or carbon black were found to accelerate the depletion of ozone, acting as initiators for the radical type chain reaction that proceed in bulk solution, leading to the transformation of ozone into secondary oxidants, such as $HO^{\bullet}$. It was suggested that the catalytic decomposition of ozone was preceded by an adsorption step on the activated carbon surface.

More recently, this subject was revisited by different authors [22-24] and the influence of both chemical and textural features of the activated carbon was evaluated.

3.1.1. Influence of the textural properties

Concerning the influence of the textural properties in the catalytic decomposition of ozone, it has been shown that activated carbons with large surface areas clearly favour this reaction [22, 23, 25]. Faria et al. [22] studied the influence of a series of modified activated carbons prepared from the same starting material and differing only in their textural properties. Strong correlations between the heterogeneous apparent rate constant (k_{Het}) and the mesopore surface area and the micropore volume were observed (see Figure 3). Nevertheless, Alvarez et al. [24] did not find any correlation between the textural properties of AC and the rate of ozone decomposition, which may be explained by the fact that the ACs tested were from different origins, possibly masking the textural effects.

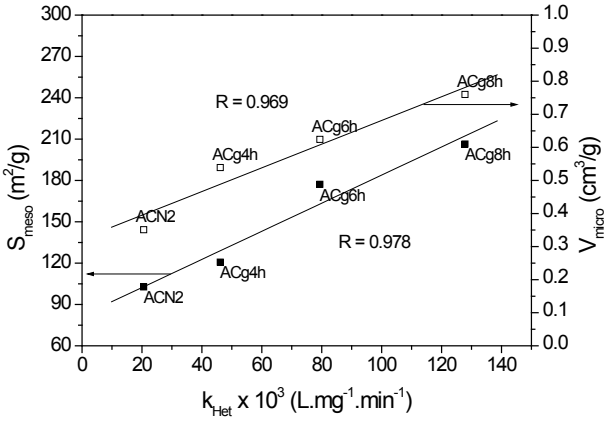

Figure 3. Variation of k_{Het} with selected textural properties of activated carbons. ACN2 is the original AC and ACgxh, where x is the duration (hours) of gasification at 900 ºC under CO_2, are the treated samples. Reprinted with permission from[22]. Copyright (2006) American Chemical Society.

Figura 3. Variación de k_{Het} con las propiedades texturales indicadas de los carbones activados. ACN2 es el AC original y ACgxh, dónde x indica la duración (horas) de gasificación a 900 ºC con CO_2, son las muestras tratadas. Reproducido con permiso de [22]. Copyright (2006) American Chemical Society.

3.1.2. Influence of the surface chemistry

It is already established that ozone decomposition is controlled by the surface chemical properties of the carbon materials, the most efficient ones being those with high basicity. Rivera-Utrilla and collaborators [15, 23] and Alvarez et al. [24] concluded that O_3 reduction on the AC surface generated OH^- ions and H_2O_2, which initiate the O_3 decomposition into highly oxidative species [26]. The delocalised π electron system (reaction 6) and the oxygenated basic surface groups, such as chromene and pyrone (reaction 7), were identified as the catalytic centres, according to the following reactions [15]:

$$O_3+H_2O+2e^- \rightleftarrows O_2+2OH^- \quad (6)$$

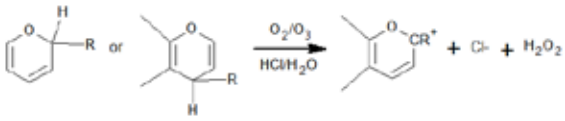

(7)

The same authors [23, 27] tested nitrogen-containing AC and concluded that pyrrolic groups were the nitrogenated active centres for O_3 decomposition. The attack of pyrrolic groups by ozone yields N-oxide-type groups and the hyperoxide radical (reaction 8), which enhances de rate of ozone transformations into hydroxyl radicals [6].

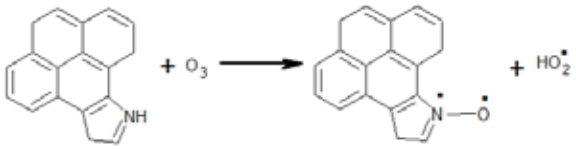

(8)

Faria et al. [22] studied the effect of pH on the catalytic decomposition of ozone and proposed that the electrostatic interactions between activated carbon surface and the solutes involved in the mechanism (including OH^- ions) may also play a role. When the pH_{pzc} of the activated carbon is higher than the pH of the solution, the surface of the material becomes positively charged, enhancing the attraction of hydroxide ions and the heterogeneous decomposition of ozone.

Successive ozone decomposition runs carried out with the same AC sample showed that the surface chemistry is mainly important in the first cycles of reaction, its effect decreasing thereafter due to a slightly progressive oxidation of the surface, which causes the increase of acidic surface groups, mainly carboxylic acids and therefore the loss of basicity [22-24]. Based on these results, Sánchez-Polo et al. and Alvarez et al. [23, 24] proposed that AC could not be a catalyst for ozone decomposition, but rather an initiator of the O_3/H_2O_2 system. Nevertheless, Faria et al. [22] concluded that basic activated carbons tended to behave as acid ACs, which were shown to still be active catalysts.

The effect of the surface chemistry of MWCNTs was recently discussed in detail in the ozone decomposition [28], and a correlation was observed between the normalized rate constant for heterogeneous ozone decomposition ($k_{d,het}/S_{BET}$) and pH_{PZC} (see Figure 4), showing that the trend of the catalytic activity for the decomposition of ozone follows the decrease of acidity, according to what was observed for activated carbons.

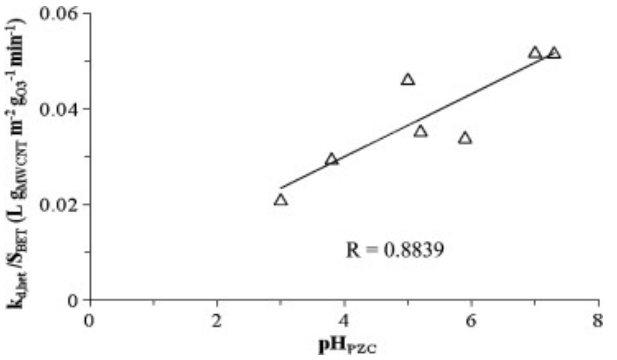

Figure 4. Correlation of the normalized rate constants for heterogeneous ozone decomposition ($k_{d,het}/S_{BET}$) with pH_{PZC}. Reproduced with permission from [28].

Figura 4. Correlación de las constantes de velocidad normalizadas para la descomposición heterogénea de ozono ($k_{d,het}/S_{BET}$) con el pH_{PZC}. Reproducido con permiso de [28].

3.2 Catalytic ozonation of organic pollutants in water

Catalytic ozonation may be included in the so-called advanced oxidation processes. These processes are based on the formation of HO· radicals, which are highly reactive towards most organic pollutants. Among these processes, the combination of ozone and carbon materials in a single step was found to be an attractive alternative to the treatment of water and wastewater containing organic contaminants. The large variety of compounds tested in this process includes small carboxylic acids, such as oxalic [29, 30], oxamic [30], pyruvic [31], and succinic acids [32], and aromatic compounds such as aniline [33], naphthalenesulfonic acid [15, 27, 34, 35], sulfonated aromatic compounds [36], phenolic compounds [37-39] and benzothiazole solutions [40]. The simultaneous use of ozone and activated carbon has been shown to be a promising method for the mineralisation of dye solutions [41-47] and for the treatment of textile wastewater [14, 41, 46-50], especially when used as a final oxidation treatment for biotreated effluents. Recently, the application of simultaneous use of ozone and activated carbon to remove emerging organic pollutants, such as EDCs and PPCPs, has been successfully investigated. The mineralization of diclofenac [51], sulphonamide antibiotics (including sulfamethoxazole [52, 53]), nitroimidazole antibiotics [54, 55] , hormones [56] and atrazine [57]) has been reported in the literature.

The scheme presented in Figure 5 summarizes the main possible reaction pathways occurring in the ozonation of organic compounds catalysed by carbon materials.

The removal of organic pollutants, as well as the respective oxidation by-products, via ozonation in the presence of carbon materials is a result of a complex combination of homogeneous and heterogeneous reactions. Both direct and indirect ozone reactions occur in the liquid phase. Additionally, reactions between adsorbed species and oxygen radicals formed on the surface of the activated carbon are assumed to occur.

Regarding the non-catalytic decomposition of ozone in aqueous solution, it is established that it is initiated by the presence of HO^- ions; so pH plays a major role in this process.

$$O_3 \xrightarrow{HO^-} HO^{\bullet} \quad (9)$$

As shown in the previous section, carbon materials accelerates the decomposition of ozone and is consensual that both textural and surface chemical properties influence that decomposition, but doubts on the mechanism still remains. Two possible pathways can explain the decomposition of O_3 in the presence of carbon materials. The first one assumes that activated carbon acts as an initiator of the decomposition of ozone, eventually through the formation of H_2O_2 [10], yielding free radical species, such as $HO^{\bullet}$, in solution [15]. Another possibility is the adsorption and reaction of ozone molecules on the surface of the activated carbon, yielding surface free radicals (O*) [12], which can react with adsorbed organic species (R*) [27]. This results in the formation of several intermediates that are further transformed into saturated compounds (P), which cannot be mineralized by direct ozone attack. Additionally, $HO^{\bullet}$ radicals in solution can also contribute to the oxidation of the organic compounds. The mineralization of the oxidation intermediates into inorganic carbon and inorganic ions (e.g. NO_3^-, NH_4^+, SO_4^{2-}), occurs both in the liquid phase through $HO^{\bullet}$ radical attack, or on the surface of the activated carbon.

Even though there is no experimental evidence, it is necessary to consider that adsorbed reactants might also react with dissolved ozone, or hydroxyl radicals from the aqueous phase [28].

It has been shown that the presence of a radical scavenger (S) induced different results depending on the organic compound studied. The effect of the radical scavenger is expected mainly when the reactions proceed in the bulk solution.

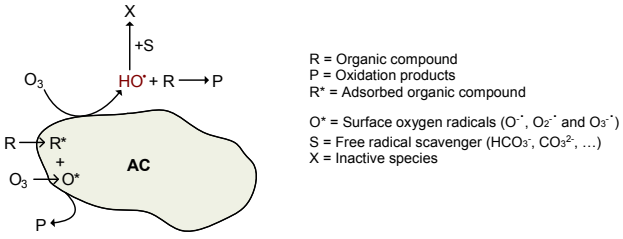

Figure 5. Schematic representation of the main reaction pathways occurring during ozonation catalysed by activated carbon (AC). Reproduced with permission from [58].

Figura 5. Esquema de las principales rutas de reacción producidas durante la ozonización catalizada con carbón activado (AC). Reproducido con permiso de [58].

Rivera-Utrilla and collaborators [15, 27, 34, 59, 60] proposed the basal plane electrons, the oxygenated basic groups (chromene and pyrone) and the pyrrole groups (in the case of N-containing samples) as the active sites responsible for ozone decomposition in aqueous phase, according to equations 6 to 8, by initiating the decomposition of O_3 into highly oxidative species, and increasing the naphthalene-1,3,6-trisulfonic acid (NTS) (an organic molecule representative of several dyes) ozonation rate [15]. They showed that the heterogeneous rate constant for NTS ozonation ($(k_{hetero})_{demi}$) was well correlated with the basicity of ACs, as can be seen in Figure 6 [59] . Similar correlation was found by Beltran at al. for the ozonation of succinic acid [32]. The advantage of the basic surface groups has also been highlighted for the catalytic ozonation of aniline [33] and different classes of dyes and textile effluents [43]. Recently, the same trend has been observed when carbon xerogels were used for the ozonation of several dyes [16] and when carbon nanotubes with different surface chemistries were used in the ozonation of oxalic and oxamic acids [28], sulfamethoxazole (SMX) [61] and bezafibrate [62].

Another additional advantage of using ozone and carbon materials simultaneously is the possibility of in-situ regeneration of the carbon material, avoiding the costly ex-situ treatment of the exhausted carbon material. This fact was observed experimentally in the catalytic ozonation of textile effluents [14] and phenol [38, 63, 64] in the presence of activated carbon.

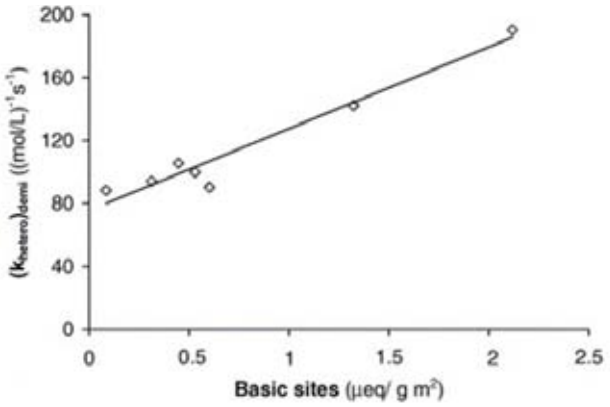

Figure 6. Relationship between the heterogeneous rate constant $(k_{hetero})_{demi}$ for the ozonation of NTS and the concentration of basic groups in demineralised ACs. Reproduced with permission from [59].

Figura 6. Relación entre la constante de velocidad heterogénea $(k_{hetero})_{demi}$ para la ozonización de NTS y la concentración de grupos básicos de ACs desmineralizados. Reproducido con permiso de [59].

3.3. Catalytic ozonation using nanocarbon materials on macrostructured catalysts.

Carbon nanotubes (CNT) and nanofibers (CNF) constitute a new family of supports offering a good compromise between the advantages of activated carbon and high surface area graphite [65]. The main drawback of activated carbons in liquid media is that they are predominantly microporous and the diffusion of solutes in this type of pores may be very slow. Diffusion limitations in the micropores of activated carbons are even more dramatic in aqueous media than in organic media due to the hydrophobic nature of carbon surface. Hence, solutes in aqueous media have hindered access to micropores, unless the surface is made hydrophilic by functionalization with e.g. oxygenated groups. In contrast, the mesoporous nature of nanocarbon materials (NCM) favours the diffusion through the pore network. Moreover, solutes have good access to mesopores of NCM, even if the pore walls are hydrophobic, i.e. without functionalization [66]. Indeed, CNTs represent an interesting alternative to conventional supports. Carbon nanotubes were barely applied as ozonation catalysts of organic pollutants. Nevertheless, the few studies found on their use in ozonation processes have reported multi-walled carbon nanotubes (MWCNT) as a very promising material. Actually, a

commercial sample of MWCNT was successfully used in the catalytic ozonation of oxalic acid [17, 67], SMX [61], bezafibrate [62] and atrazine [68]. Similarly to activated carbon, the mechanism involves a combination of bulk and surface reactions.

Most of the mentioned studies use nanocarbon catalysts in the powder form, which is a problem for their practical application in water treatment. A solution to overcome this drawback is to grow these nanomaterials onto a macrostructure. In this way, it is possible to enhance oxidation in catalytic ozonation by facilitating mass transfer across the different phases, and the ease of operation associated to a macrostructure is seen as a very important advantage of this technology. The process eliminates the need for filtration of catalyst particles, while reducing pressure drop when compared to packed bed reactors.

An example of this type of macrostructure catalyst is shown in Figure 7 [69]. It consists of a commercial honeycomb cordierite structure, upon which CNFs were grown after coating the monolith with an alumina wash coat impregnated with nickel, which acts as a catalyst for carbon growth. In this particular case, CNFs were formed under a gas flow of ethane and hydrogen (50:50) at 600 ºC.

The utilization of this type of structured catalysts in continuous ozonation experiments has been already applied in the removal of oxalic acid as well as several emerging organic micropollutants (atrazine, bezafibrate, erythromycin, metolachlor and nonylphenol) with very promising results [69-71].

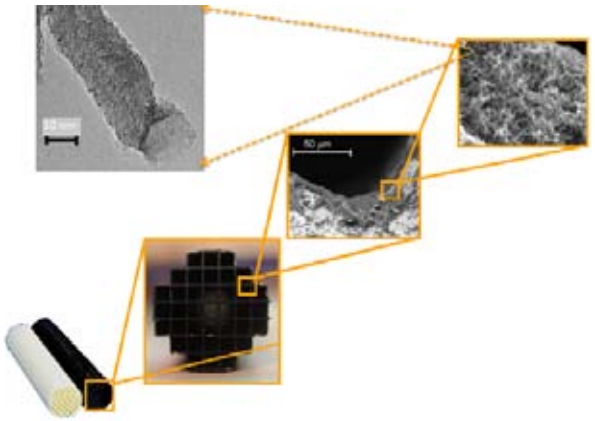

Figure 7. Honeycomb monolith covered with CNFs used in the catalytic ozonation of emerging organic pollutants. Reproduced with permission from [69].

Figura 7. Monolitos de panal de abeja recubiertos con CNFs usados en la ozonización catalítica de contaminantes orgánicos emergentes. Reproducido con permiso de [69].

4. Conclusions

Intensive research has been carried out on the ozonation of several organic pollutants in the presence of carbon materials. Two catalytic pathways may occur simultaneously: 1) decomposition of O_3 into $HO^{\bullet}$ or other highly active oxygen-containing radicals on the surface of the carbon materials, with sequent oxidation in the homogeneous phase; and 2) adsorption of the organic compounds on carbon, which then react on the surface with O_3 or oxygenated radicals. Therefore, the surface chemistry of carbon samples plays a key role in the catalytic ozonation of organic pollutants. In general, catalytic ozonation is favoured by carbons with basic or neutral properties. Recently, the use of carbon nanofibers and nanotubes supported on macrostructures (like monoliths or foams) has been appointed as a very promising system, since it overcomes the problem of mass transfer resistances usually observed in the case of microporous materials.

5. Acknowledgements

This work was partially supported by the European Community's Seventh Framework Programme (FP7/2007-2013) under Grant Agreement No. 280658, by FEDER through COMPETE (project PEst-C/EQB/LA0020/2013), and by QREN, ON2 and FEDER (Project NORTE-07-0124-FEDER-0000015). A. G. acknowledges the Grant received from FCT (BD/45826/2008).

6. References

[1] Oyama ST. Chemical and catalytic properties of ozone. Cat Rev 2000; 42(3):279-322.

[2] Beltrán FJ. Ozone reaction kinetics for water and wastewater systems. Boca Raton, Florida: Lewis Publishers. 2004.

[3] Hoigné J. Chemistry of ozone and transformation of pollutants by ozonation and advanced oxidation processes. In: Hubrec J, editor. The handbook of environmental chemistry Vol 5, Part C, Quality and treatment of drinking water II. Weinheim: Wiley-VCH; 1998.

[4] Buxton GV, Greenstock CL, Helman WP, Ross AB. Critical review of rate constants for the reaction of hydrated electrons, hydrogen atoms and hydroxyl radicals (·OH/·O⁻) in Aqueous Solution. J Phys Chem Ref Data 1988; 17(0):513-886.

[5] Weiss J. Investigations on the radical HO_2 in solution. Trans Faraday Society 1935; 31(0):668-81.

[6] Staehelin J, Hoigné J. Decomposition of ozone in water: Rate of initiation by hydroxide ions and hydrogen peroxide. Environ Sci Technol 1982; 16(10):676-81.

[7] Sotelo JL, Beltran FJ, Benitez FJ, Beltran-Heredia J. Ozone decomposition in water: kinetic study. Ind Eng Chem Res 1987; 26(1):39-43.

[8] von Gunten U. Ozonation of drinking water: Part I. Oxidation kinetics and product formation. Water Res 2003; 37(7):1443-67.

[9] Hoigné J, Bader H. Rate constants of reactions of ozone with organic and inorganic compounds in water - I: Non-dissociating organic compounds. Water Res 1983; 17(2):173-83.

[10] Hoigné J. Inter-calibration of OH radical sources and water quality parameters. Water Sci Technol 1997; 35(4):1-8.

[11] Kasprzyk-Hordern B, Ziólek M, Nawrocki J. Catalytic ozonation and methods of enhancing molecular ozone reactions in water treatment. Appl Catal B: Environ 2003; 46(4):639-69.

[12] Legube B, Karpel Vel Leitner N. Catalytic ozonation: a promising advanced oxidation technology for water treatment. Catal Today 1999; 53(1):61-72.

[13] Beltrán FJ, Rivas FJ, Montero-de-Espinosa R. Catalytic ozonation of oxalic acid in an aqueous TiO_2 slurry reactor. Appl Catal B: Environ 2002; 39(3):221-31.

[14] Lin SH, Lai CL. Kinetic characteristics of textile wastewater ozonation in fluidized and fixed activated carbon beds. Water Res 2000; 34(3):763-72.

[15] Rivera-Utrilla J, Sánchez-Polo M. Ozonation of 1,3,6-naphthalenetrisulphonic acid catalysed by activated carbon in aqueous phase. Appl Catal B: Environ 2002; 39(4):319-29.

[16] Orge CA, Sousa JPS, Gonçalves F, Freire C, Órfão JJM,

Pereira MFR. Development of novel mesoporous carbon materials for the catalytic ozonation of organic pollutants. Catal Lett 2009; 132(1):1-9.

[17] Liu Z-Q, Ma J, Cui Y-H, Zhang B-P. Effect of ozonation pretreatment on the surface properties and catalytic activity of multi-walled carbon nanotube. Appl Catal B: Environ 2009; 92(3-4):301-6.

[18] Ma J, Sui M, Zhang T, Guan C. Effect of pH on MnOx/GAC catalyzed ozonation for degradation of nitrobenzene. Water Res 2005; 39(5):779-86.

[19] Sánchez-Polo M, Rivera-Utrilla J, von Gunten U. Metal-doped carbon aerogels as catalysts during ozonation processes in aqueous solutions. Water Res 2006; 40(18):3375-84.

[20] Liu Z-Q, Ma J, Cui Y-H. Carbon nanotube supported platinum catalysts for the ozonation of oxalic acid in aqueous solutions. Carbon 2008; 46(6):890-7.

[21] Jans U, Hoigné J. Activated carbon and carbon black catalyzed transformation of aqueous ozone into OH radicals. Ozone Sci Eng 1998; 20(1):67-90.

[22] Faria PCC, Órfão JJM, Pereira MFR. Ozone decomposition in water catalysed by activated carbon: influence of chemical and textural properties. Ind Eng Chem Res 2006; 45(8):2715-21.

[23] Sánchez-Polo M, von Gunten U, Rivera-Utrilla J. Efficiency of activated carbon to transform ozone into OH radicals: Influence of operational parameters. Water Res 2005; 39(14):3189-98.

[24] Alvárez PM, García-Araya JF, Beltrán FJ, Giráldez I, Jaramillo J, Gómez-Serrano V. The influence of various factors on aqueous ozone decomposition by granular activated carbons and the development of a mechanistic approach. Carbon 2006; 44(14):3102-12.

[25] Guiza M, Ouerdeni A, Ratel A. Decomposition of dissolved ozone in the presence of activated carbon: An experimental study. Ozone Sci Eng 2004; 26(3):299-307.

[26] Gurol MD, Singer PC. Kinetics of ozone decomposition: A dynamic approach. Environ Sci Technol 1982; 16(7):377-83.

[27] Rivera-Utrilla J, Sánchez-Polo M. Ozonation of naphthalenesulphonic acid in the aqueous phase in the presence of basic activated carbons. Langmuir 2004; 20(21):9217-22.

[28] Gonçalves AG, Figueiredo JL, Órfão JJM, Pereira MFR. Influence of the surface chemistry of multi-walled carbon nanotubes on their activity as ozonation catalysts. Carbon 2010; 48(15):4369-81.

[29] Béltran FJ, Rivas FJ, Fernandez LA, Alvarez PM, Montero-de-Espinosa R. Kinetics of catalytic ozonation of oxalic acid in water with activated carbon. Ind Eng Chem Res 2002; 41(25):6510-7.

[30] Faria PCC, Órfão JJM, Pereira MFR. Activated carbon catalytic ozonation of oxamic and oxalic acids. Appl Catal B: Environ 2008; 79(3):237-43.

[31] Beltrán FJ, Acedo B, Rivas FJ, Gimeno O. Pyruvic acid removal from water by the simultaneous action of ozone and activated carbon. Ozone Sci Eng 2005; 27(2):159-69.

[32] Beltrán FJ, García-Araya JF, Giráldez I, Masa FJ. Kinetics of activated carbon promoted ozonation of succinic acid in water. Ind Eng Chem Res 2006; 45(9):3015-21.

[33] Faria PCC, Órfão JJM, Pereira MFR. Ozonation of aniline promoted by activated carbon. Chemosphere 2007; 67(4):809-15.

[34] Sánchez-Polo M, Rivera-Utrilla J. Effect of the ozone–carbon reaction on the catalytic activity of activated carbon during the degradation of 1,3,6-naphthalenetrisulphonic acid with ozone. Carbon 2003; 41(2):303-7.

[35] Rivera-Utrilla J, Sánchez-Polo M. Degradation and removal of naphthalenesulphonic acids by means of adsorption and ozonation catalyzed by activated carbon in water. Water Resour Res 2003; 39(9):1-13.

[36] Faria PCC, Órfão JJM, Pereira MFR. Catalytic ozonation of sulfonated aromatic compounds in the presence of activated carbon. Appl Catal B: Environ 2008; 83(1-2):150-9.

[37] Beltrán FJ, García-Araya JF, Giráldez I. Gallic acid water ozonation using activated carbon. Appl Catal B: Environ 2006; 63(3-4):249-59.

[38] Lin SH, Wang CH. Ozonation of phenolic wastewater in a gas-induced reactor with a fixed granular activated carbon bed. Ind Eng Chem Res 2003; 42(8):1648-53.

[39] Giráldez I, García-Araya JF, Beltrán FJ. Activated carbon promoted ozonation of polyphenol mixtures in water: Comparison with single ozonation. Ind Eng Chem Res 2007; 46(24):8241-7.

[40] Valdés H, Zaror CA. Heterogeneous and homogeneous catalytic ozonation of benzothiazole promoted by activated carbon: Kinetic approach. Chemosphere 2006; 65(7):1131-6.

[41] Soares OSGP, Faria PCC, Orfao JJM, Pereira MFR. Ozonation of textile effluents and dye solutions in the presence of activated carbon under continuous operation. Sep Sci Technol 2007; 42(7):1477-92.

[42] Kawasaki N, Ogata F, Yamaguchi I, Fujii A. Removal of orange II, methylene blue and humic acid by ozone-activated carbon combination (OZAC) treatment. J Oleo Sci 2008; 57(7):391-6.

[43] Faria PCC, Órfão JJM, Pereira MFR. Mineralisation of coloured aqueous solutions by ozonation in the presence of activated carbon. Water Res 2005; 39(8):1461-70.

[44] Gul S, Bahar G, Yildirim OO. Comparison of ozonation and catalytic ozonation processes for the decolourization of reactive red 195 azo dye in aqueous solution. Asian J Chem 2010; 22(5):3885-94.

[45] Gul S, Ozcan O, Erbatur O. Ozonation of CI Reactive Red 194 and CI Reactive Yellow 145 in aqueous solution in the presence of granular activated carbon. Dyes Pigm 2007; 75(2):426-31.

[46] Gul S, Eren O, Kir S, Onal Y. A comparison of different activated carbon performances on catalytic ozonation of a model azo reactive dye. Water Sci Technol 2012; 66(1):179-84.

[47] Faria PCC, Órfão JJM, Pereira MFR. Activated carbon and ceria catalysts applied to the catalytic ozonation of dyes and textile effluents. Appl Catal B: Environ 2009; 88(3-4):341-50.

[48] Arsian-Alaton I, Seremet O. Advanced treatment of biotreated textile industry wastewater with ozone, virgin/ozonated granular activated carbon and their combination. J Environ Sci Health, Pt A: Toxic/Hazard Subst Environ Eng 2004; 39(7):1681-94.

[49] Arslan-Alaton I. Granular activated-carbon assisted ozonation of biotreated dyehouse effluent. AATCC Review 2004; 4(5):21-4.

[50] Alvarez PM, Beltran FJ, Masa FJ, Pocostales JP. A comparison between catalytic ozonation and activated carbon adsorption/ozone-regeneration processes for wastewater treatment. Appl Catal B: Environ 2009; 92(3-4):393-400.

[51] Beltrán FJ, Pocostales P, Alvarez P, Oropesa A. Diclofenac removal from water with ozone and activated carbon. J Hazard Mater 2009; 163(2-3):768-76.

[52] Beltrán FJ, Pocostales P, Alvarez PM, Lopez-Pineiro F. Catalysts to improve the abatement of sulfamethoxazole and the resulting organic carbon in water during ozonation. Appl Catal B: Environ 2009; 92(3-4):262-70.

[53] Pocostales JP, Alvarez PM, Beltran FJ. Kinetic modeling of powdered activated carbon ozonation of sulfamethoxazole in water. Chem Eng J 2010; 164(1):70-6.

[54] Sánchez-Polo M, Rivera-Utrilla J, Prados-Joya G, Ferro-García MA, Bautista-Toledo I. Removal of pharmaceutical compounds, nitroimidazoles, from waters by using the ozone/carbon system. Water Res 2008; 42(15):4163-71.

[55] Rivera-Utrilla J, Sánchez-Polo M, Prados-Joya G, Ferro-García MA, Bautista-Toledo I. Removal of tinidazole from waters by using ozone and activated carbon in dynamic regime. J Hazard Mater 2010; 174(1-3):880-6.

[56] Beltran FJ, Pocostales P, Alvarez P, Aguinaco A. Ozone-activated carbon mineralization of 17α-ethynylestradiol aqueous solutions. Ozone Sci Eng 2009; 31(6):422-7.

[57] Guzman-Perez CA, Soltan J, Robertson J. Kinetics of catalytic ozonation of atrazine in the presence of activated carbon. Sep Purif Technol 2011; 79(1):8-14.

[58] Figueiredo JL, Pereira MFR. The role of surface chemistry in catalysis with carbons. Catal Today 2010; 150(1–2):2-7.

[59] Sanchez-Polo M, Leyva-Ramos R, Rivera-Utrilla J. Kinetics of 1,3,6-naphthalenetrisulphonic acid ozonation in presence of activated carbon. Carbon 2005; 43(5):962-9.

[60] Sánchez-Polo M, Rivera-Utrilla J. Ozonation of naphthalenetrisulphonic acid in the presence of activated carbons prepared from petroleum coke. Appl Catal B: Environ 2006; 67(1–2):113-20.

[61] Gonçalves AG, Órfão JJM, Pereira MFR. Catalytic ozonation of sulfamethoxazole in the presence of carbon materials: catalytic performance and reaction pathways. J Hazard Mater 2012; 239-240(0):167-74.

[62] Gonçalves A, Órfão JJM, Pereira MFR. Ozonation of bezafibrate promoted by carbon materials. Appl Catal B: Environ 2013; 140–141(0):82-91.

[63] Polaert I, Wilhelm AM, Delmas H. Phenol wastewater treatment by a two-step adsorption-oxidation process on activated carbon. Chem Eng Sci 2002; 57(9):1585-90.

[64] Qu X, Zheng J, Zhang Y. Catalytic ozonation of phenolic wastewater with activated carbon fiber in a fluid bed reactor. J Colloid Interface Sci 2007; 309(2):429-34.

[65] Serp P. Carbon nanotubes and nanofibers in catalysis. In: Serp P, Figueiredo JL, editors. Carbon materials for catalysis. New Jersey: Jonh Wiley & Sons, Inc.: Hoboken; 2009.

[66] Job N, Sabatier F, Pirard J-P, Crine M, Léonard A. Towards the production of carbon xerogel monoliths by optimizing convective drying conditions. Carbon 2006; 44(12):2534-42.

[67] Liu Z-Q, Ma J, Cui Y-H, Zhao L, Zhang B-P. Influence of different heat treatments on the surface properties and catalytic performance of carbon nanotube in ozonation. Appl Catal B: Environ 2010; 101(1-2):74-80.

[68] Fan X, Restivo J, Órfão JJM, Pereira MFR, Lapkin AA. The role of multiwalled carbon nanotubes (MWCNTs) in the catalytic ozonation of atrazine. Chem Eng J 2014; 241(0):66-76.

[69] Restivo J, Órfão JJM, Armenise S, Garcia-Bordejé E, Pereira MFR. Catalytic ozonation of metolachlor under continuous operation using nanocarbon materials grown on a ceramic monolith. J Hazard Mater 2012; 239-240(0):249-56.

[70] Restivo J, Orfao JJM, Pereira MFR, Garcia-Bordeje E, Roche P, Bourdin D, Houssais B, Coste M, Derrouiche S. Catalytic ozonation of organic micropollutants using carbon nanofibers supported on monoliths. Chem Eng J 2013; 230(0):115-23.

[71] Restivo J, Órfão JJM, Pereira MFR, Vanhaecke E, Rönning M, Iouranova T, Kiwi-Minsker L, Armenise S, Garcia-Bordejé E. Catalytic ozonation of oxalic acid using carbon nanofibres on macrostructured supports. Water Sci Technol 2012; 65(10):1854-62.

Photooxidation reactions promoted by the photochemical activity of nanoporous carbons

Reacciones de fotooxidación basadas en materiales de carbono nanoporosos

L. F. Velasco[1,2], C. O. Ania[1]

[1] Dpt. Chemical Processes for Energy and Environment, Instituto Nacional del Carbón (INCAR), CSIC, Oviedo 33080, España (conchi.ania@incar.csic.es)

[2] Dpt. Chemistry, Royal Military Academy, Renaissancelaan 30, 1000 Brussels, Belgium (leticia.fernandez@rma.ac.be)

1. Broader context

After the early works in 1960's and 70`s reporting the photochemistry of ZnO and TiO_2 electrodes and their potential application in water splitting and environmental remediation [1,2], heterogeneous photocatalysis has become a popular topic. However, the low photonic efficiency of most semiconductors is still a challenge, thus optimizing the optical features of semiconductor materials remains a largely investigated topic [3,4]. Addressing these problems calls out for a research to be conducted to enhance the performance of semiconductors or to explore the possible use of other types of materials in this kind of applications. Among different approaches, the incorporation of carbon materials in the formulation of hybrid photocatalysts seems an interesting strategy to attain high photoconversion efficiencies. First investigations in the field focused on the use of carbons as supports and additives of TiO_2, and the enhanced photocatalytic performance of carbon/TiO_2 composites has been attributed to several factors associated to visible light absorption and the porosity of the carbon support, and/or strong interfacial electronic effects [5-8]. More recently, our pioneering studies have demonstrated the self-photochemical activity of semiconductor-free nanoporous carbons [9,10], along with their ability to generate O-radical species upon irradiation [11,12]. Despite the increasing interest of the topic, there is yet a dearth in the understanding of the role of carbons in photo-assisted reactions and the underlying mechanisms leading to the conversion of light into a chemical reaction (i.e. photooxidation of pollutants). By combining catalytic, spectroscopic and photoelectrochemical tools, we herein provide an overview of the photochemical response of nanoporous carbons applied to environmental remediation.

2. The role of carbon materials on photocatalysis

Triggered by the rising interest in heterogeneous photocatalysis, numerous efforts have been made in the last decades to improve the optical properties of semiconductor materials. Among different strategies, novel hybrid materials prepared by immobilization of the photoactive semiconductor on appropriate substrates have gained increased interest due to the superior performance observed on such composites [5,8,13-17]. Despite carbons are strong light absorbing materials, they have also been extensively

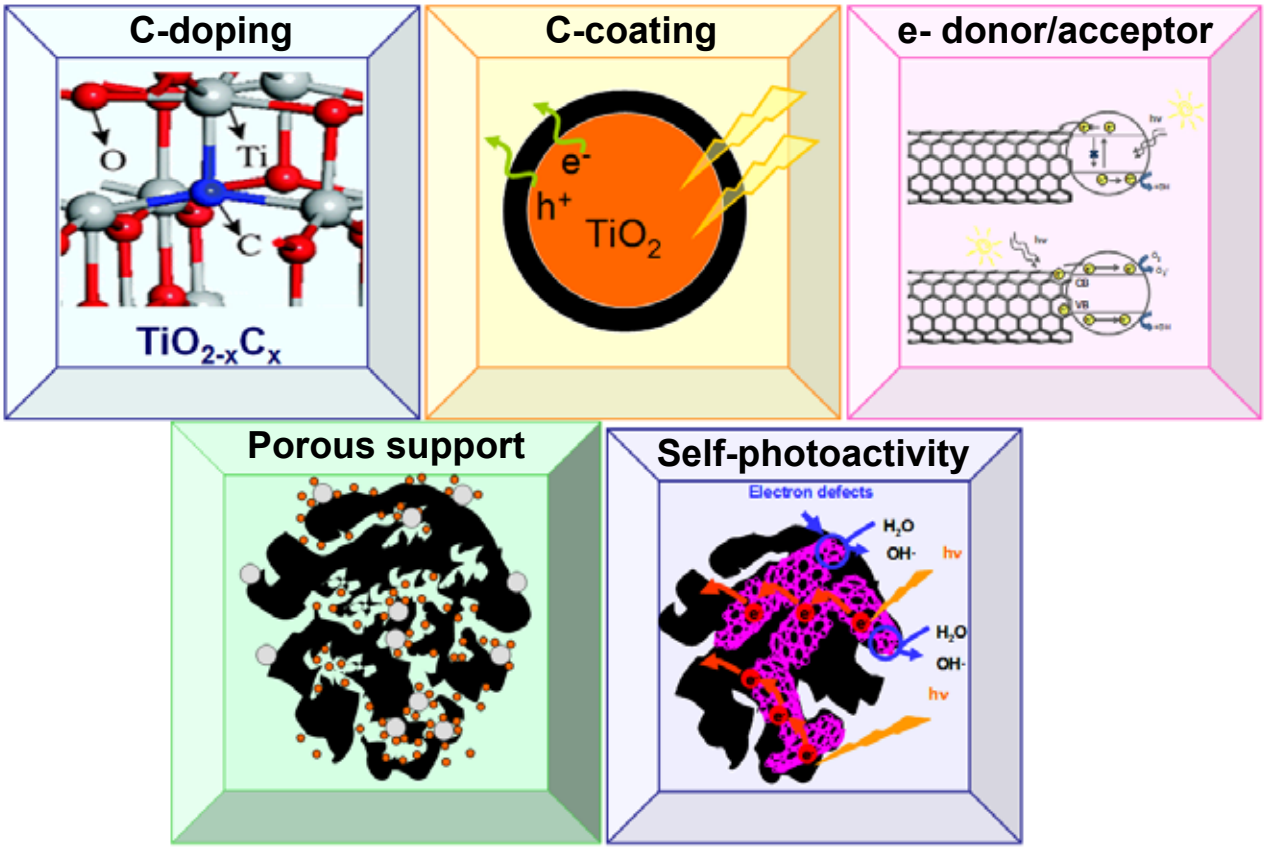

Figure 1. Sketch illustrating the role of carbon materials in photocatalysis.

Figura 1. Esquema ilustrativo del empleo de materiales de carbono en fotocatálisis.

investigated in a number of photo-assisted reactions [5-7 and references therein]. The majority of the studies deal with the use of carbon/semiconductor composites, where the carbon material acts either as a dopant or a support of the photoactive material (Fig. 1).

For instance, metallic and non-metallic doping seems a promising route to extend the optical absorption of conventional semiconductors towards the visible region, allowing the use of sunlight [18-22]. Comparatively, non-metallic doping is considered to be more effective than transition metal doping due to the high photostability and lack of photocorrosion of the resulting catalyst. Furthermore, the isomorphic incorporation of carbon atoms in the lattice of semiconductors is considered to be more effective than other non-metal heteroatoms. Most authors agree to explain this effect in terms of the redshift in the absorption properties of doped material and the modifications in the electronic band structure of the metal oxide associated to band gap narrowing and localized midgap levels [21,22].

Besides semiconductor-doping, the incorporation of nanoporous carbons as supports in hybrid carbon/semiconductor composites is another interesting alternative to prepare efficient photocatalysts. The idea, firstly introduced by Matos et al. [8], relies on the combination of the confinement of the pollutant in the porosity of the catalyst via adsorption with the photoactivity of the semiconductor. After this early work based on activated carbons, a variety of carbon sources, forms and morphologies have been explored, using from conventional (activated carbon, carbon black, graphites) to novel carbons (nanotubes, graphene), as well as different synthetic routes for the catalyst preparation (physical mixture, liquid impregnation, hydrothermal process, chemical vapor deposition) [5-7]. The increased photoconversion yields of carbon/semiconductor composites has been ascribed to the enhanced mass transfer of the adsorbed pollutant from the bulk solution to the photoactive particles through the interface between the two catalyst components, and to the interactions between the substrate and the

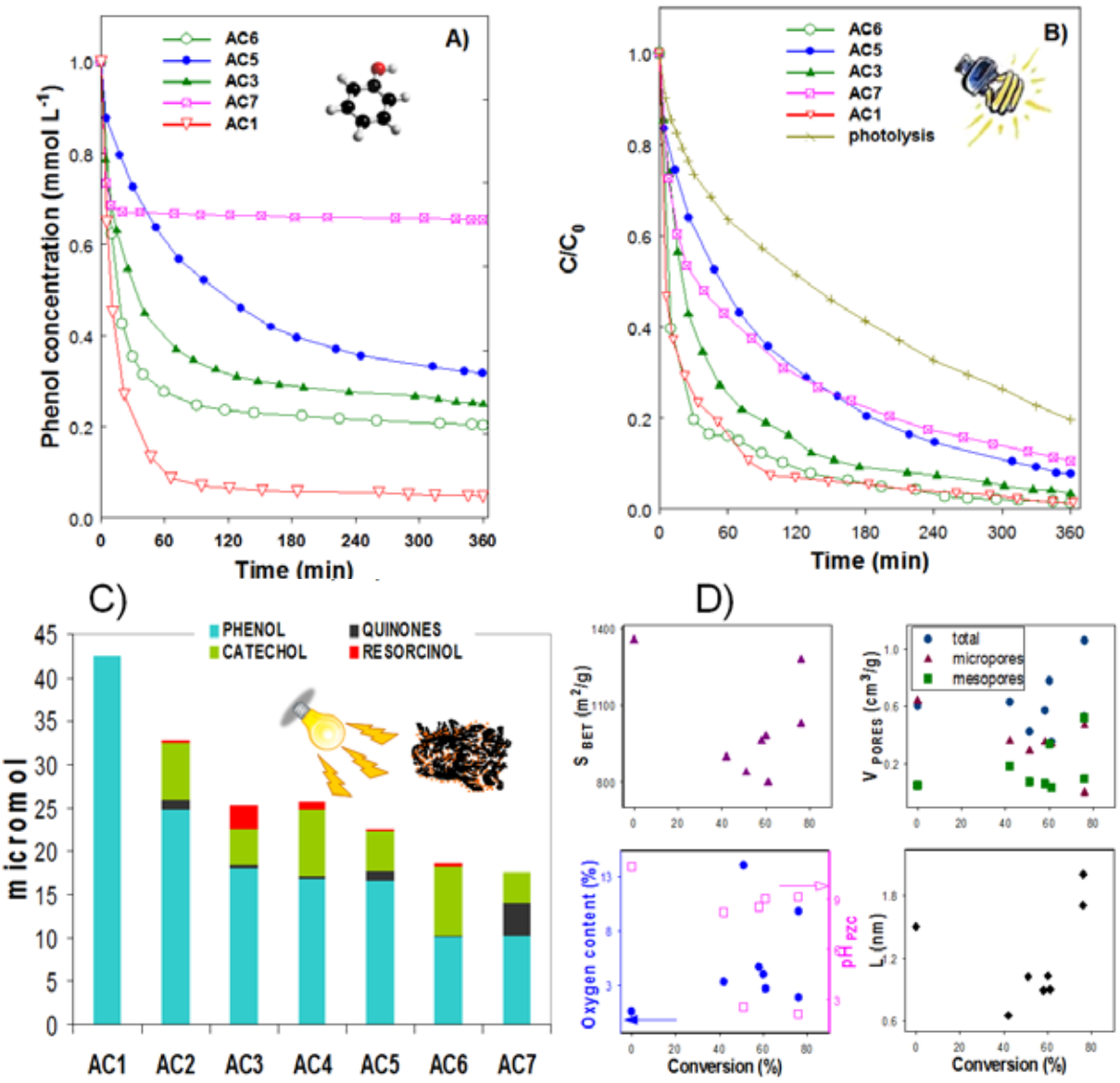

Figure 2. (top) Phenol concentration decay curves on selected carbons after (A) dark adsorption and (B) UV irradiation. (**down)** Phenol photooxidation and intermediates speciation upon irradiation of pre-loaded carbons (C) and correlation with selected characteristics of the nanoporous carbons (D).

Figura 2. (arriba) Evolución de la concentración de fenol con el tiempo en presencia de los fotocatalizadores estudiados durante (A) adsorción en oscuridad y (B) irradiación con luz UV. **(abajo)** Conversion de fenol e intermedios de oxidación tras la irradiación de los carbones pre-adsorbidos con fenol (C) y correlación de la conversion de fenol con algunas características físico-químicas de los materiales de carbono empleados (D).

immobilized catalyst [14,17]. Also, it is considered that the photocatalytic enhancement depends greatly on the nature of the carbon matrix itself, hence different mechanisms would apply for nanoporous carbons compared to nanostructured carbon nanotubes, fullerenes and graphene. Furthermore, the use of carbon/semiconductor composites overcomes the operational drawbacks associated to the use of nanosized semiconductor powders -that hinder the application in continuous flow systems due to limited recovery and reuse of the catalyst- [16].

3. Self-photoactivity of nanoporous carbons

Our recent investigations have shown the self-photochemical activity of nanoporous carbons under UV irradiation, with improved photooxidation conversions in aqueous solution compared to bare or carbon-immobilized titania [10-12,23]. Data showed that beyond the synergistic effect of carbon/TiO_2 composites, the nanoporous carbon alone was capable of a significant level of self photo-activity under UV irradiation (Fig. 2).

Upon UV irradiation the overall rate of phenol disappearance increased remarkably for all the nanoporous carbons, particularly at the initial stage of the reaction and for those materials showing an acidic nature. The relative abundance of the degradation intermediates detected in solution was also dependent on the characteristics of the carbons, with a marked regioselectivity for the formation of catechol over quinones (as opposed to titania). Such regioselectivity is considered more advantageous for the overall reaction yield as it proceeds through a less number of subproducts. [24].

Although the self photoactivity of multiwall carbon nanotubes under visible light had been reported and attributed to the presence of structural defects and vacancies [25], amorphous nanoporous carbons had been considered merely as inert supports to enhance the photoactivity of semiconductor materials [5-8,14-17,26]. Several possible scenarios were considered to explain our findings: (1) adsorption/desorption of the photooxidation intermediates; (2) concentration effect on photolysis; (3) occurrence of carbon/light interactions and degradation of the adsorbed compounds retained in the inner porosity. Differences in conversion (rate and intermediates speciation) under dark and UV irradiation cannot be explained by the nanoconfinement of the pollutant (scenario 2) in the porosity (i.e., concentration effect on photolysis). Also, adsorption of the degradation intermediates (scenario 1) cannot account for the unbalance between the amount of compounds detected in solution and that retained in the porosity after the photocatalytic runs. To demonstrate if the UV light can somehow interact with the compounds retained inside the porosity of the carbons (scenario 3), the reaction was monitored from inside the carbonaceous matrix.

4. Photocatalytic evidences on preloaded samples

To determine the extent of phenol photodegradation (if any) inside the carbons, irradiation was performed on carbon samples pre-loaded with phenol, thereby disregarding the effects of adsorption kinetics and solution photolysis [10]. The concentration of phenol and intermediates was exclusively detected after extraction of the carbons with solvents; data obtained for different preloaded carbons are shown in Fig. 2C. As no leaching out occurred during the irradiation, these results demonstrate that a fraction of phenol is decomposed inside the porosity of the carbons when these are illuminated.

The distribution and nature of the intermediates detected was different for the studied carbons. It is also interesting to note that for most carbons, phenol photodegradation was larger or similar than in the photolytic reaction. This is most remarkable since the incident photo flux arriving at the phenol molecules adsorbed inside the carbons porosity is expected to be smaller than that from solution. However, this singular photochemical behavior does not apply for all type of carbon adsorbents since one of the studied carbons showed negative response. No straightforward correlation has been found so far between the photochemical response of these carbons towards phenol degradation and their physicochemical and/or structural features in terms of porosity, composition and surface acidity/basicity (Fig. 2D).

These results demonstrated that a fraction of the adsorbed molecules are decomposed when certain nanoporous carbons are exposed to UV light, although it is not yet clear whether if the UV light penetrates inside the carbons porosity or if interactions occur at the external surface and are subsequently propagated through the graphene sheets. Anyhow, such carbon/photons interactions could promote the formation of charge carriers that seem to have enough redox potential to generate more reactive species (radicals) and/or directly oxidize phenol (scenario 3). To determine the occurrence of the carbon/light interactions, a deep investigation was undertaken by combining spectroscopic and photoelectrochemical tools.

5. Spectroscopic evidences

To shed light on the origin of the photochemical response of semiconductor-free nanoporous carbons and to establish the likely formation of radical species upon illumination, we have carried out spin resonance spectroscopy (ESR) studies [11,12]. The formation of paramagnetic species in solution upon irradiation of carbon suspensions was detected by a nitrone spin trapping agent (DMPO).

The ESR spectra of all the samples (Fig. 3) showed a quartet peak profile with 1:2:2:1 intensity, assigned to DMPO-OH adducts [27]. Some other adducts, identified as HDMPO-OH, DMPO-R (carbon centered radical) and DMPO-OOH, were also detected. Our results demonstrate that significant amounts of •OH and/or superoxide anion radicals are formed during the irradiation of the nanoporous carbons in the absence of semiconductor additive, likely produced from photoinduced oxidation of water. Quantification of the relative abundance of the radical species showed that the DMPO-OH concentration levels measured for certain carbons were higher than those obtained for titania, indicating a higher concentration of radical species. Among the investigated carbons, as a general rule lower ESR signals were obtained for those materials showing a rich surface chemistry. On the other hand, only for one of the studied carbons no

radicals were detected, which seemed in agreement with the lack of photoactivity observed for this material in previous works [10]. ESR patterns are a diagnostic indication of free hydroxyl radical formation in aqueous environments, and may constitute a key issue on the understanding of the photochemical response of carbon materials. Nevertheless, low ESR signals should not be considered as an indication of low photoactivity, as this technique only provides information about the formation of radicals under irradiation. Indeed, for certain materials low ESR signals corresponded to high photooxidation yields and viceversa [11,12]. This would indicate either a radical-mediated or a direct hole oxidation as dominating pathways.

6. Photoelectrochemical evidences

Further insights on the mechanisms occurring at the carbon/semiconductor interfaces when these are exposed to light were obtained by investigating the optoelectronic and photoelectrochemical response of carbon/titania thin film electrodes of increasing carbon content ranging from 5-50 wt.% [28]. Voltammetric techniques were used to study the effect of potential bias on the photocurrent response of the different carbon/titania catalysts (Fig. 4). In the dark, the shape of the current-potential curves of the carbon/titania electrodes was similar to that of a titania electrode, with small capacitive contribution due to the non negligible porosity of the carbon matrix. The characteristic shape of n-type semiconductor was detected, with the distinctive accumulation and depletion regions (below/above -300 mV sv SCE, respectively). Upon UV illumination, anodic photocurrents were observed in all studied electrodes when the bias potential was positive enough for an efficient hole-electron separation. As opposed to titania, no photocurrent saturation limit was observed for the carbon/titania electrodes, particularly for those with the highest carbon content.

The transient photoamperometric curves upon on-off illumination for several bias potentials (Fig. 4c) showed a similar trend. On switching-on the light, an initial sharp current spike is followed by a steady-state regime, which retracted to original values almost instantaneously once the illumination was turned off. In the absence of hole scavengers other than water, this photocurrent corresponds to water oxidation. The photocurrent response was rapid and reproducible during repeated on/off cycles of illumination, for which the initial current decay is attributed to fast recombination processes rather than to photocorrosion of the electrodes. Interestingly, the carbon/titania thin film electrodes showed roughly similar photocurrent values than those of TiO_2 films. Additionally, the photocurrent enhancement after phenol addition to the electrolytic solution, indicative of direct hole oxidation, was clearly observed for all the thin film electrodes.

The high photocurrents measured in the composites are related to a higher density of photogenerated electrons recovered at the back contact of the electrical circuit likely as a result of an efficient charge carrier separation; this indicates that the incorporation of the carbon additive plays an

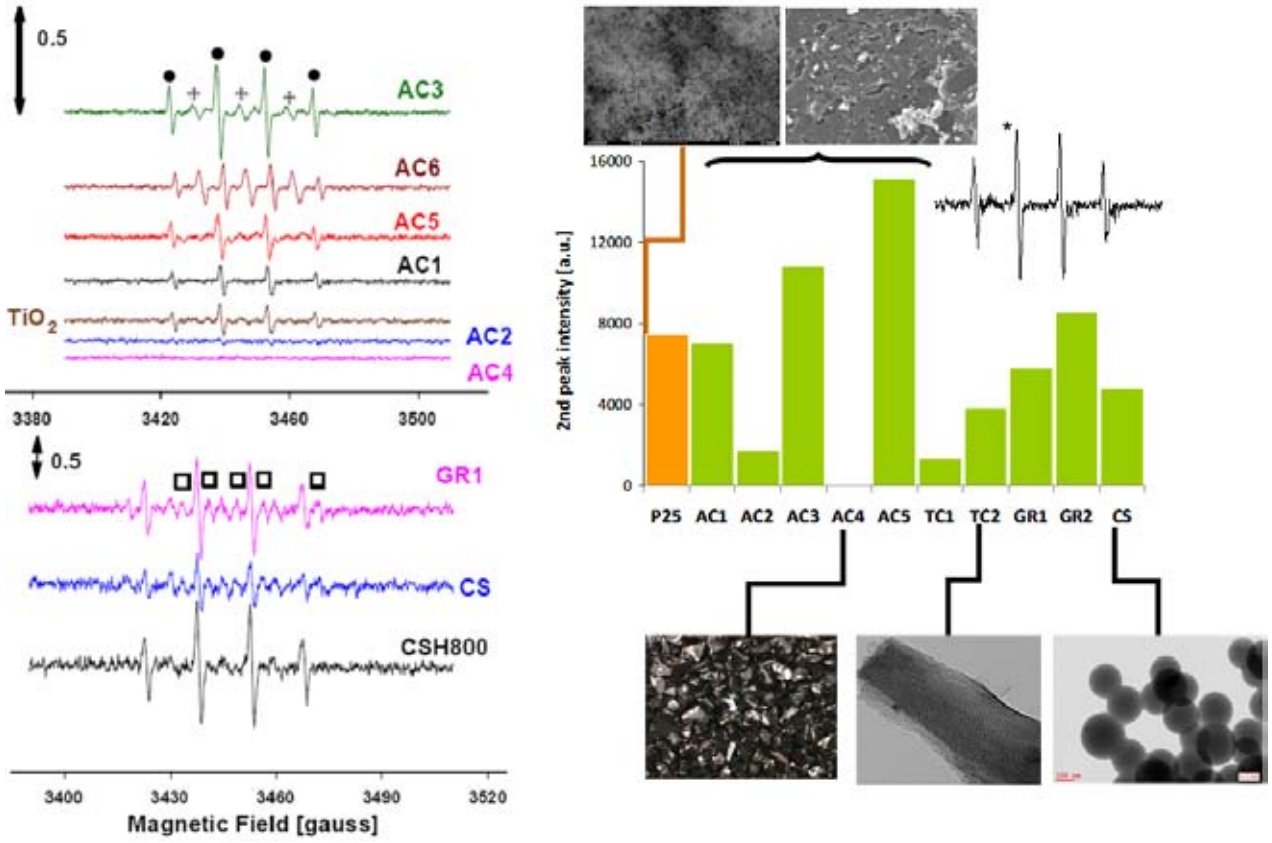

Figure 3. (left) ESR spectra of the DMPO adducts obtained after 20 minutes irradiation of aqueous suspension of semiconductor-free nanoporous carbons and TiO_2. Assignments to DMPO-OH (circles), HDMPO-OH (diamonds) and DMPO-OR (squares) adducts are indicated. **(right)** Quantification of the radical species determined from the intensity of the second line (asterisk in inset) of the ESR spectra.

Figura 3. (izquierda) Espectros de RPE de los aductos de DMPO tras 20 minutos de irradiación de suspensions acuosas de materiales de carbono y TiO_2. Las especies detectadas son: DMPO-OH (círculos), HDMPO-OH (rombos) y DMPO-OR (cuadrados). **(derecha)** Cuantificación de las especies radicalarias detectadas a partir de la integración de la intensidad del segundo pico (marcado con un asterisco) de los espectros de RPE.

important role for the photoelectrochemical response of the composites, and anticipates a potentially higher photocatalytic activity of these materials. The gathered results showed that the incorporation of the porous carbon matrix to the titania film electrodes favors the probability of charge transfer reactions at the porous carbon/titania interface by several likely mechanisms (Fig 4):

i) the smaller diffusion length of the carriers through the porous structure provided by the carbon material (favoring photohole capture and indirect oxidations).

ii) the carbon matrix can act as an acceptor of the photogenerated electrons upon UV irradiation of the titania particles; the delocalization and stabilization of the carriers within the graphene layers of the carbon additive would contribute to minimize the surface recombination.

iii) photon absorption by the carbon material itself, generating charge carriers due to direct $\pi-\pi^*$ and/or $\sigma-\pi*$ transitions, contributing to increased photocurrents.

7. Cycleability and performance under long illumination periods

Beyond establishing the origin of the photochemical behavior of activated carbons, it becomes essential to explore their performance during consecutive photodegradation runs, and determine if they fulfill the requirements of long cycle life, and good degradation efficiency. To attain this goal, we have carried out the photocatalytic degradation of phenol from solution upon 20 hours of illumination in consecutive cycles, using two nanoporous carbons with different surface chemistry [29]. The performance was also compared to commercial TiO_2 under similar illumination conditions. Given the porous nature of the carbons, the experiments incorporated a pre-adsorption step at dark conditions -before the illumination- to control the amount of pollutant adsorbed on the carbons, and hence maintaining the same phenol concentration in solution at the beginning of each cycle for the nanoporous carbons and the semiconductor [29]. Data showed that, under excess of oxygen, the overall performance of the nanoporous carbons upon cycling was comparable to that of commercial titania, with close mineralization yields in all three studied materials after six consecutive cycles. For both studied carbons, a marked accumulation of phenol degradation intermediates was observed during cycling, with preferential formation of catechol over quinones. For titanium oxide, the concentration of aromatic intermediates was lower but still the total organic carbon values showed a quite low mineralization due to the accumulation of short alkyl chain organic acids. The photocatalytic efficiency was found to depend strongly on the basic/acidic nature of the nanoporous carbons, with a somewhat lower

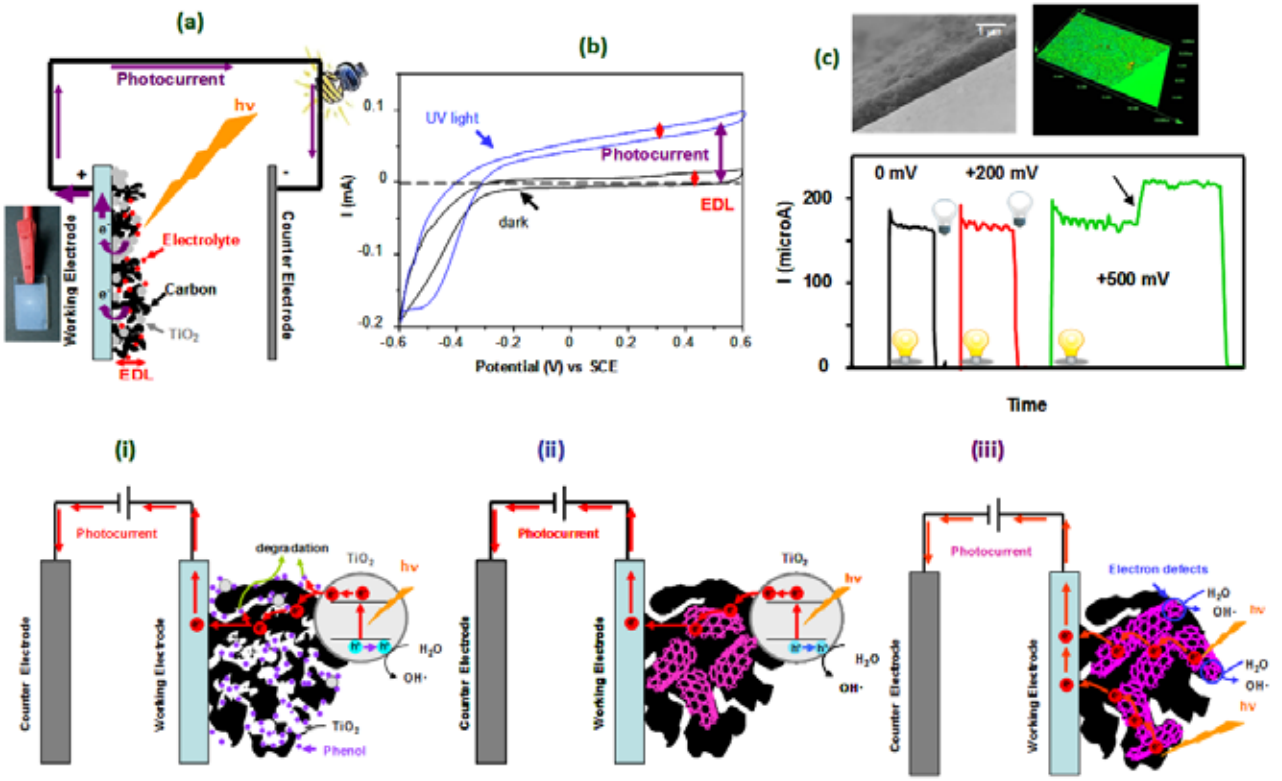

Figure 4. (top) a) Sketch of the experimental set-up used for the photoelectrochemical measurements; b) Representative potential-current curves under dark and UV light of a carbon/titania thin film electrode; c) Chronoamperometric response of the film electrodes upon on/off illumination cycles in the supporting electrolyte and in the presence of phenol (arrow) at various fixed bias potentials (vs SCE) of a carbon/titania composite. Representative images of the thin film electrodes, obtained by SEM and confocal microscope are also included. **(down)** Scheme of the mechanisms proposed for illustrating the role of carbon in the photocatalytic performance of carbon/titania interfaces: (i) diffusion length of carriers, (ii) carbon as acceptor of photogenerated electrons, (iii) photon absorption by the carbon material.

Figura 4. (arriba) a) Esquema del dispositivo experimental utilizado para las medidas fotoelectroquímicas; b) Curvas de intensidad-potencial en condiciones de oscuridad y bajo radiación UV con un electrodo C/TiO_2 de película fina; c) Respuesta cronoamperométrica de un electrodo C/TiO_2 en oscuridad/irradiación en presencia de electrolito y fenol (flecha) a varios potenciales. También se muestran imágenes de los electrodos de película fina obtenidas por SEM y microscopía confocal. **(abajo)** Esquema de los mecanismos propuestos para la interpretación de la influencia del material de carbono en la respuesta de los electrodos C/TiO_2: (a) difusión de los portadores de carga en la porosidad del material de carbono, (b) material de carbono como aceptor de los electrones fotogenerados en el TiO_2, (c) absorción de fotones por el material de carbono.

performance for the hydrophilic catalysts. Phenol conversion and mineralization rates were greatly enhanced in the presence of excess of dissolved oxygen in the solution, demonstrating the outstanding role of oxygen in the photooxidation of phenol. This was critical for the long-term performance of the hydrophilic carbon, which showed a sharp fall in phenol conversion upon cycling under oxygen depletion conditions.

8. Acknowledgements

The authors thank the financial support of the Spanish MINECO (grants CTM2008/01956, CTM2011/02338) and PCTI Asturias (Fondos Feder 2007-2013, grant PC10-002).

9. References

[1] Barry TI, Stone FS. The reactions of oxygen at dark and irradiated zinc oxide surface. Proc. Royal Soc. 1960;255:124-44.

[2] Fujishima A, Honda K. Electrochemical photolysis of water at a semiconductor electrode. Nature 1972;238:37-8.

[3] Henderson MA. A surface science perspective on TiO_2 photocatalysis. Surf. Sci. Rep. 2011;66:185-297.

[4] Serpone N, Pelizzetti E. Photocatalysis: fundamental and applications, New York: Wiley Interscience; 1989.

[5] Leary R, Westwood A. Carbonaceous nanomaterials for the enhancement of TiO_2 photocatalysis. Carbon 2011;49:741-72.

[6] Faria JL, Wang W. Carbon materials in photocatalysis. In: Serp P, Figueiredo JL, editors. Carbon materials for catalysis, New York; John Wiley & Sons; 2009, p. 481-506.

[7] Ania CO, Velasco LF, Valdes-Solis T. Photochemical response of carbon materials. In: Tascon JMD, editor. Novel Carbon Adsorbents, London; Elsevier; 2012, p. 521-47.

[8] Matos J, Laine J, Herrmann JM. Synergy effect in the photocatalytic degradation of phenol on a suspended mixture of titania and activated carbon. Appl. Catal. B: Environ 1998;18:281-91.

[9] Velasco LF, Parra JB, Ania CO. Role of activated carbon features on the photocatalytic degradation of phenol. Appl. Surf. Sci. 2010;256:5254-8.

[10] Velasco LF, Fonseca IM, Parra JB, Lima JC, Ania CO. Photochemical behaviour of activated carbons under UV irradiation. Carbon 2012;50:249-58.

[11] Velasco LF, Maurino V, Laurenti E, Ania CO. Light-induced generation of radicals on semiconductor-free carbon photocatalysts. Appl. Catal A: Gen 2013;453:310-5.

[12] Velasco LF, Maurino V, Laurenti E, Fonseca IM, Lima JC, Ania CO. Photoinduced reactions occurring on activated carbons. A combined photooxidation and ESR study. Appl Catal A: Gen 2013;452:1-8

[13] Fernández A, Lassaletta G, Jiménez VM, Justo A, González-Elipe AR, Herrmann JM, Tahiri H, Ait-Ichou Y. Preparation and characterization of TiO_2 photocatalysts supported on various rigid supports (glass, quartz and stainless steel). Comparative studies of photocatalytic activity in water purification. Appl. Catal. B Environ. 1995;7:49-63.

[14] Torimoto T, Ito S, Kuwabata S, Yoneyama H. Effects of adsorbents used as supports for titanium dioxide loading on photocatalytic degradation of propyzamide. Environ. Sci. Technol. 1996;30:1275-81.

[15] Velasco LF, Tsyntarski B, Petrova B, Budinova T, Petrov N, Parra JB, Ania CO. Carbon foams as catalyst supports for phenol photodegradation. J. Haz. Mat. 2010;184:843-8.

[16] Araña J, Doña-Rodríguez JM, Tello Rendón E, Garriga i Cabo C, González-Díaz O, Herrera-Melián JA, Pérez-Peña J, Colón G, Navío JA. TiO_2 activation by using activated carbon as a support. Part I. Surface characterisation and decantability study. Appl. Catal. B: Environ. 2003;44:161-72.

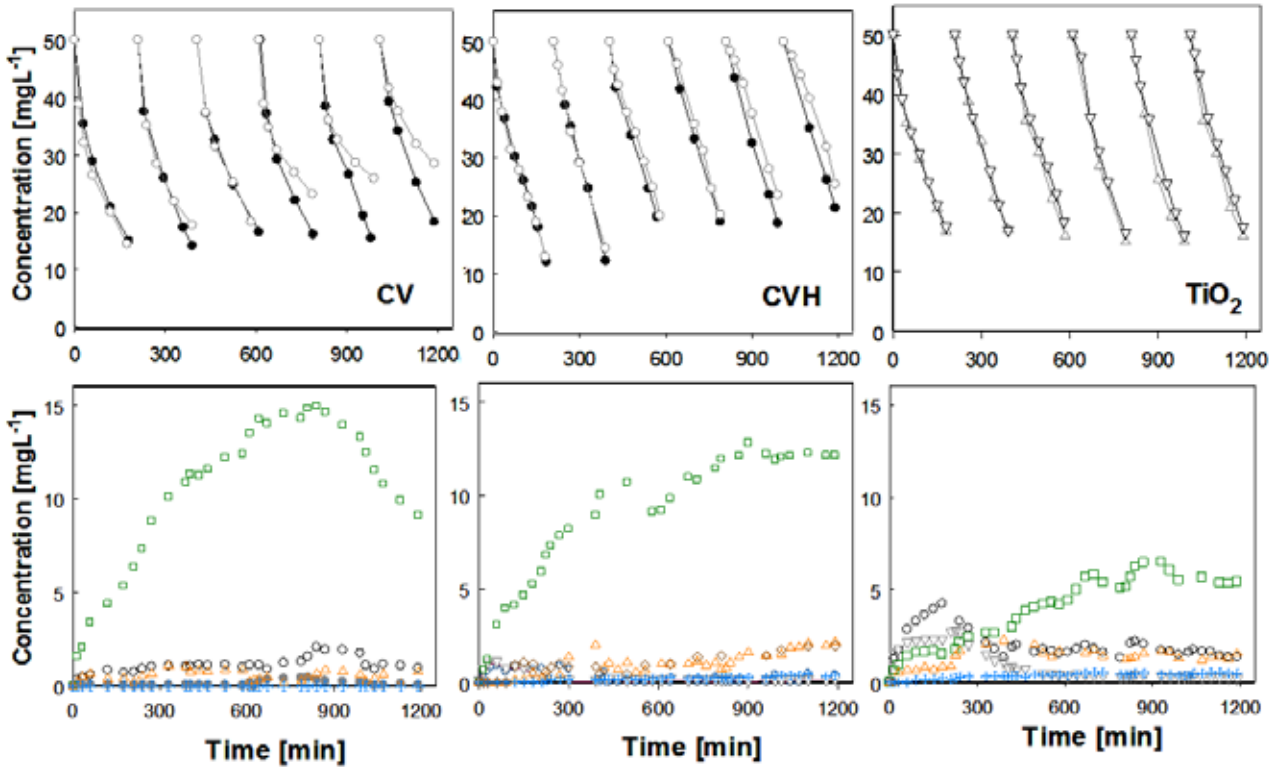

Figure 5. (top) Evolution of phenol concentration upon consecutive photocatalytic runs in the presence of nanoporous carbons and titania, under excess (solid symbols) and depleted (empty symbols) oxygen conditions. **(down)** Evolution of degradation intermediates: hydroquinone (circles); benzoquinone (down triangles); cathecol (squares); 2,4,6-trihydroxybenzene (up triangles); resorcinol (crosses); 1,3,5-trihydroxybenzene (diamonds).

Figura 5. (arriba) Evolución de la concentración de fenol durante 6 ciclos fotocatalíticos consecutivos empleando carbones activados y TiO_2 como catalizadores y en condiciones de exceso (símbolos llenos) y defecto (símbolos huecos) de oxígeno disuelto. **(abajo)** Evolución de intermedios de degradación: hidroquinona (círculos); benzoquinona (triángulos invertidos); catecol (cuadrados); 2,4,6-trihidroxibenceno (triángulos); resorcinol (cruces); 1,3,5-trihidroxibenceno (rombos).

[17] Keller N, Rebmann G, Barraud E, Zahraa O, Keller V. Macroscopic carbon nanofibers for use as photocatalyst support. Catal. Today 2005;101:323-9.

[18] Llano B, Restrepo G, Marin JM, Navio JA, Hidalgo MC. Characterisation and photocatalytic properties of titania-silica mixed oxides doped with Ag and Pt. Appl. Catal. A General 2010;387:135-40.

[19] Litter MI, Navio JA. Photocatalytic properties of iron-doped titania semiconductors. J. Photochem. Photobiol. A, Chem 1996;98:171-81.

[20] Minero C, Mariella G, Maurino V, Pelizzetti E. Photocatalytic transformation of organic compounds in the presence of inorganic anions. 1. Hydroxyl-mediated and direct electron-transfer reactions of phenol on a titanium dioxide-fluoride system. Langmuir 2000;16:2632-41.

[21] Sakthivel S, Kisch H. Daylight photocatalysis by carbon-modified titanium dioxide. Angew. Chem. Int. Edit. 2003;42:4908-11.

[22] Di Valentin C, Pacchioni G, Selloni A. Theory of carbon doping of titanium dioxide. Chem. Mater. 2005;17:6656-65.

[23] Velasco LF. Fotodegradación oxidativa de fenol con catalizadores TiO_2-C. Análisis de la respuesta fotoquímica de la fase carbonosa. University of Oviedo, PhD thesis, 2012.

[24] Santos A, Yustos P, Quintanilla A, Rodríguez S, Garcia-Ochoa F. Route of the catalytic oxidation of phenol in aqueous phase. Appl Catal B: Environ 2002;39:97-113.

[25] Luo Y, Heng Y, Dai X, Chen W, Li J. Preparation and photocatalytic ability of highly defective carbon nanotubes. J. Solid State Chem. 2009;182:2521-5.

[26] Matos J, Chovelon JM, Cordero T, Ferronato C. Influence of surface properties of activated carbon on photocatalytic activity of TiO_2 in 4-chlorophenol degradation. Open Environ. Eng. J. 2009;2:21-9.

[27] Finkelstein E, Rosen GM, Rauckman E. Spin trapping. Kinetics of the reaction of superoxide and hydroxyl radicals with nitrones. J. Arch. Biochem. Biophys. 1980;200:1-16.

[28] Haro M, Velasco LF Ania CO. Carbon-mediated photoinduced reactions as a key factor in the photocatalytic performance of C/TiO_2, Catal. Sci. Tech. 2012;2:2264-72.

[29] Velasco LF, Carmona RJ, Matos J, Ania CO. Performance of activated carbons in consecutive phenol photooxidation cycles. Carbon (in press, dx.doi.org/10.1016/j.carbon.2014.02.056).

Socios protectores del Grupo Español del carbón

Industrial Química del Nalón, S.A.
NalónChem

TECNOVAC
TECNOLOGÍA DE VACÍO S.L.

GRONTAL